Major Project-II

CFD Analysis of Single Phase Turbulent Flow with Forced Convection Heat Transfer inside a Circular Microchannel

Submitted in Partial Fulfillment

of the Requirements for the Award of the Degree of

Master of Technology
In
Thermal Engineering

Submitted By

Amit Kumar

2K13/THE/04

Under the Guidance of

Dr. Raj Kumar Singh

Associate Professor

Department of Mechanical Engineering

Delhi Technological University

(Formerly Delhi College of Engineering)

Shahabad-Daulatpur, Bawana Road, Delhi-110042

DECLARATION

I hereby declare that the work, which is being presented in this dissertation, entitled **"CFD Analysis of single phase turbulent flow with forced convection heat transfer inside a circular microchannel"** towards the partial fulfillment of the requirements for the award of the degree of Master of Technology with specialization in Thermal Engineering, from Delhi Technological University Delhi, is an authentic record of my own work carried out under the supervision of **DR. RAJ KUMAR SINGH** Associate Professor, Department of Mechanical Engineering, at Delhi Technological University, Delhi.

The matter embodied in this dissertation report has not been submitted by me for the award of any other degree.

Amit Kumar
2K13/THE/04
Place: Delhi
Date:

This is to certify that the above statement made by the candidate is correct to the best of my knowledge.

DR. RAJ KUMAR SINGH
Associate Professor
Department of Mechanical Engineering
Delhi Technological University
Delhi-110042

CERTIFICATE

It is certified that Amit Kumar, Roll no. 2K13/THE/04, student of M.Tech, Thermal Engineering, Delhi Technological University, has submitted the dissertation titled entitled **" CFD Analysis of single phase turbulent flow with forced convection heat transfer inside a circular microchannel "** under my guidance towards the partial fulfillment of the requirements for the award of the degree of Master of Technology.

DR. RAJ KUMAR SINGH
Associate Professor
Department of Mechanical Engineering
Delhi Technological University
Delhi-110042

ACKNOWLEDGEMENT

Generally, individuals set aims, but more often than not, their conquest are by the efforts of not just one but many determined people. This complete project could be accomplished because of contribution of a number of people. I take it as a privilege to appreciate and acknowledge the efforts of all those who have, directly or indirectly, helped me achieving my aim.

I take great pride in expressing my unfeigned appreciation and gratitude to my guide, DR. RAJ KUMAR SINGH, Associate Professor, Department of Mechanical Engineering, for his invaluable inspiration, guidance, and continuous encouragement throughout this project work.

Amit Kumar
2K13/THE/04

ABSTRACT

For many years, several experiments have been conducted to analyze the fluid flow and heat transfer parameters in microchannel heat sinks which are designed for applications in electronic cooling. These microchannels provide high surface area per unit volume and large potential for heat transfer. The present work addresses and investigates the study of a single-phase water cooled circular microchannel heat sink for electronic packages with forced convection of water by the help of a commercial CFD software FLUENT. The geometry of the problem and meshing has been done in ANSYS Workbench. The models of the problem have been solved by Fluent solver. In this report, a computational fluid dynamics (CFD) model for fully developed turbulent flow (k-ϵ model) has been implemented with the help of FLUENT 14.5 software.

In the present work Nusselt number has been calculated for the given flow conditions and the result has been compared with the results of T.M.ADAMS' experimental work. The hydrodynamic and thermal behaviour of the system have been studied in terms of velocity, pressure and temperature contours. Variation of temperature and pressure along centerline, outlet temperature variation and wall shear profile have been plotted. Axial velocity profile and temperature profiles at three different locations have been compared. In the present work simulation has been done for microchannel with diameter 0.76mm and 1.09mm with water as a coolant. Simulation has also been done for microchannel of diameter 0.76mm diameter with air as the coolant.

Key words: *microchannel, heat sink, Nusselt Number, CFD, velocity, temperature, pressure, FLUENT.*

Table of Contents

List of Figures

Circular Microchannel of 1.09mm Diameter

Simulation of Microchannel of 0.76mm Diameter with Air as a Coolant

NOMENCLATURE

Symbols

A	area of cross-section
Cp	specific heat
Dh	hydraulic diameter
f	friction factor
k	thermal conductivity
V	velocity
μ	dynamic viscosity
ρ	density
q"	heat flux
Gk	generation of turbulence K.E due to mean velocity gradient
Gb	generation of turbulence K.E due to buoyancy
Ym	fluctuating dilatation in compressible turbulence to the overall dissipation rate
C1ξ	constant = 1.44
C2ξ	constant = 1.92
C3ξ	constant = 0.09
σ k	turbulent Prandtl number for K
σr	turbulent prandtl number for ξ
Sk	user defined source term
Sξ	user defined source term

Non-Dimensional Numbers

Re	Reynolds Number
Nu	Nusselt Number
Pr	Prandtl Number

Abbreviations

VLSI	very large integration
CFD	computational fluid dynamics

1. INTRODUCTION

1.1 General

Recently a lot of developments have taken place in the field of VLSI technology and MEMS. These demand electronic chips to be manufactured which are embedded with microchannel. The thermal energy developed during the operation of these chips needs to be dissipated by providing microchannel on these chips. It has been found that the main reason for the failure of chips is primly due to accumulation of heat. So microchannel embedded chips comes as a feasible and efficient solution of this problem. These microchannel combined with forced convection cooling ensures effective and proper working of these electronic chips. Thus these electronic chips serve as heat sink. These heat sinks have been categorized into single phase and two-phase depending upon whether boiling takes place inside the microchannel or not. The primary factors that determine single phase and double phase flow are heat flux on the wall of microchannel and the coolant flow rate. Low flow rate of coolant may result in boiling of the coolant and hence it will be considered as two phase flow.

Microchannels find its applications in, microprocessors, radars, laser diode arrays and high energy laser mirrors [1]. For the same Re number and hydraulic diameter, rectangular channels have lower thermal resistance while circular microchannels dissipate more heat per unit pumping power [2].

The trend towards higher circuit density got accompanies by more and more heat production which demanded increased power dissipation rate. The demand of increased packaging density of chips led to substantial increment in heat flux.

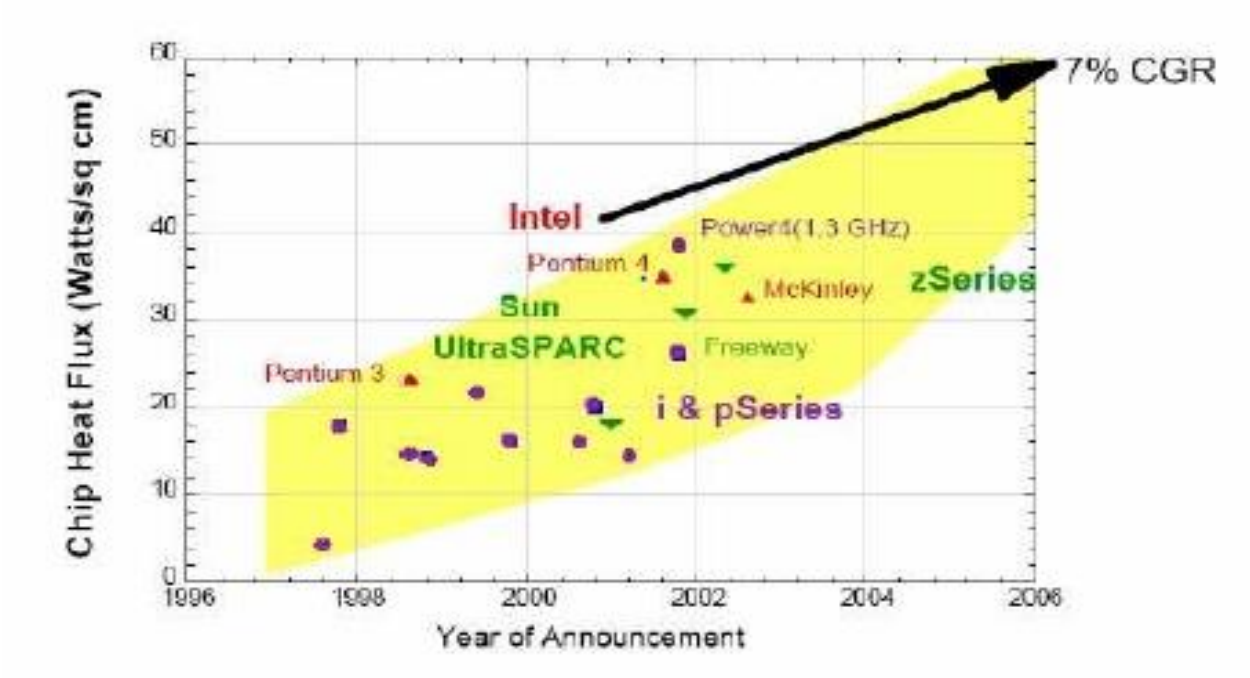

Fig.1.1 The chronological evolution of chip level heat flux [3]

The main reason for the failure of electronic chip is temperature rise (55%) while other factors contributing to chip failure are vibration (20%), humidity (19%) and dust (6%).

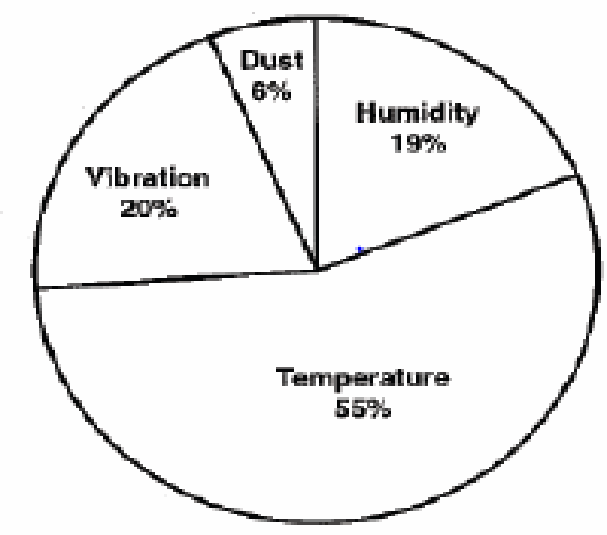

Fig. 1.2 Major causes of electronics failure [4]

1.2 Cooling Methods Used in Industries

Different methods used in electronic industries for cooling modules, systems and data centers are as follows:

1.2.1 Module Level Cooling

It is done in two ways i.e; cooling external and internal surface of chip module.

1.2.1.1 Internal Module Cooling

The mode of heat transfer in this method is by conduction. The internal thermal resistance is determined by construction of modules and physical properties. Heat is transferred from internal surface to the outer surface by conduction which can be further removed by different methods.

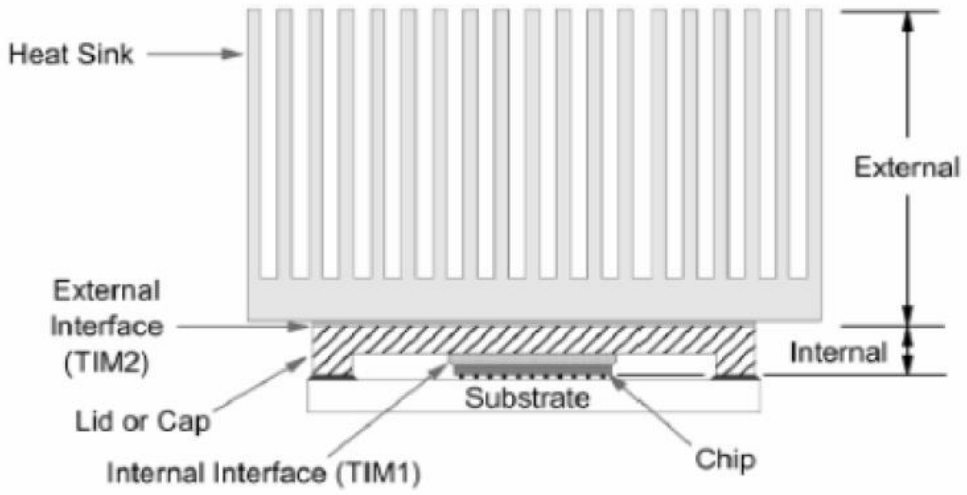

Fig. 1.3 Cross-section of a typical module denoting internal cooling region and external cooling region [5]

1.2.1.2 External Module Cooling

In this method a heat sink is attached to the module which is cooled by air or some other means. Preferably it is done by air because of availability and low cost.

1.2.1.3 Immersion Cooling

In immersion cooling coolant is brought in direct contact of the chip. Liquid ammonia is generally used for this purpose which provides high heat transfer coefficient. The mode of heat transfer in this process includes natural convection, forced convection and boiling as well.

1.2.2 System Level Cooling

In this system like computers are cooled by different methods which are as follows:

1.2.2.1 Air Cooling

In this method air is used and the mode of heat transfer is forced convective heat transfer that cools the electronic modules and packages. The rate of cooling is controlled by varying rate of flow.

1.2.2.2 Hybrid Cooling

In this system, hot air is cooled by heat exchanger which in turn is cooled by water. Here the module is still cooled by air only but the heated air is cooled by water cooled heat exchanger. Generally finned tube heat exchanger is used for this purpose.

1.2.2.3 Liquid Cooling System

Electronic chips or packaging is enclosed inside a frame around which a closed loop is made. This loop forms the primary loop through which water runs in and out of the frame. This primary loop is cooled by a secondary loop running water through it.

1.2.2.4 Refrigeration Cooled System

In this type of system the electronic packaging is cooled by a loop or channel, running refrigerant through it.

1.3 Heat Sink

It is an environment that absorbs heat and thereby helps other systems in dissipating heat.

Applications of heat sink:

1. It finds its application in cooling electronic devices like microprocessors etc.
2. It is of great use in Refrigeration.
3. One of classic example of heat sink is heat engines.

1.4 Microchannel Heat Sink

With advancement of microelectronics heat removal becomes of great importance. This is due to integrated density of chips and increased current and voltage handling capacity of these devices.

The heat removing capacity of microchannel is 50 times higher than conventional heat sinks. These microchannel induce thermal stresses on the system which are being cooled. In order to avoid these thermal stresses large pressure drop is required which further needs a pumping system. Several improvements have taken in the field of microchannel. One of such example is multilayered microchannel. The main advantage of multilayered microchannel is that it needs less pressure drop across the microchannel and it offers less thermal resistance as well. Obot in 2003 gave a simpler classification which is based on hydraulic diameter.

According to his classification channel whose hydraulic diameter is less than 1mm is called microchannel. Hydraulic diameter can be defined as

$D_h = 4A \div P;$

Where A = area

P = perimeter

D_h = hydraulic diameter

Microchannels provide one of the alternatives to finned tube heat exchanger. Microchannel heat sinks are usually made of material of high thermal conductivity such as copper and silicon using precision machining of micro machining processes. Microchannel is actually composed of a number of parallel micro channels and coolant is forced through this microchannel. It is the coolant that takes away heat from the heated surface. Advantages of using microchannel are as follows:

1. It provides large surface area to volume ratio.
2. It facilitates a high value of convective heat transfer coefficient.
3. It has small mass and volume.
4. It requires less inventory.

Because of these merits microchannels are well suited as heat sink for devices like high performance micro processors, laser diode array, radars and high energy laser mirrors.

1.5 ASSUMPTIONS:

(a) Steady state heat conduction.

(b) No heat generation within the microchannel.

(c) Uniform heat transfer coefficient over the entire surface of the microchannel.

(d) Homogeneous and isotropic microchannel material (i.e. thermal conductivity of material constant).

(e) Negligible contact thermal resistance.

(f) Heat conduction one-dimensional.

(g) Negligible radiation

(h) Thickness of microchannel is negligible and is placed horizontally.

(i) Density of the coolant is constant.

2. LITERATURE REVIEW

2.1 Introduction

Some experimental and theoretical work on micro channel heat exchanger has been done in the last decades. Both the industrial and academic people have taken interest in this area. This chapter can be broadly classified under three categories. The first part of the survey deals with analytical studies. The second part of the survey deals with the experimental studies and the third part of the survey deals with the numerical studies. The following is a review of the research that has been completed especially on microchannel heat exchangers. The literature review is arranged according to similarity to the work done in this report.

2.2 Analytical Study of Fluid Flow and Heat Transfer in Microchannels

Y. S. Muzychka [6] analyzed constructional design of forced convection cooled microchannel heat sink and heat exchanger in 2005. He examined heat transfer from arrays of circular and non circular duct subjected to finite volume and constant pressure drop. He concluded that optimal duct dimension is independent of array structure. He presented the solution for optimal duct dimension and maximum heat transfer per unit volume for the parallel plate channel, rectangular channel, elliptical duct, polygon ducts and rectangular ducts. Approximate analytical results show that the optimal shape is the isosceles right triangle and square duct due to their ability to provide the most efficient packing in a fixed volume. Whereas a more exact analysis reveals that the parallel plate channel array is in fact the superior system. An approximate relationship is developed which is very nearly a universal solution for any duct shape in terms of the Bejan number and duct aspect ratio.

Ravindra Kumar, Mohd. Islam and M.M. Hasan [7] reviewed experimental investigation on heat transfer characteristics of single phase liquid flow in microchannel in 2014. In this paper heat transfer characteristics of single phase liquid flow in microchannel by different researchers has been reviewed and discrepancies and possible causes between experimental observation and theoretical predictions have been analyzed. It has also been observed that nano-fluids as coolant in microchannel have excellent potential to enhance heat transfer performance establishing as future coolant.

Sambhaji T. Kadam and Ritunesh Kumar [8] suggested microchannel heat sink as 21st century cooling solution. In his paper experimental studies on flow visualization, pressure drop and heat transfer characteristics of microchannel by different researchers have been summarized. The influence of vapour quality, heat flux, mass flux and channel geometry on pressure drop and heat characteristics of microchannel have been reported. Different correlations for single phase and two phase heat transfer characteristics have been compared.

2.3 Experimental Study of Fluid Flow and Heat Transfer in Microchannels

Microchannel heat sink was first proposed for heat sinking of VLSI electronic components in 1980s. **Tuckerman and Pease [9]** used silicon microchannels, with water as the working fluid, to dissipate power from an electronic chip. The microchannels were etched in a silicon sample with an overall dimension of 1cm2. They had a channel width of approximately 60 μm and a parameterized channel height varying between 287 μm and 376 μm. These microchannels effectively dissipated heat up to 790 W/cm^2 while maintaining a chip temperature below 110 °C.

Wong and Peck [10] evaluated experimentally the effect of altitude on electronic cooling. As material properties of air vary as a function of altitude due to changes in atmospheric pressure and temperature, these changes have a negative impact on the heat transfer effectiveness and result in higher component temperature when compared to sea level conditions. They carried out the experiments in a hypobaric chamber using electronic printed circuit boards populated with heated rectangular blocks placed in a small wind tunnel. The altitude was varied between 0 and 5000 m above sea level and the air speed is varied between 1 and 5 m/s. The results show the local adiabatic heat transfer coefficient and thermal wake function diminish with altitude. This information is useful for design and analysis of electronic equipment for operation over a range of altitudes and air speeds typically encountered in forced air convection cooling applications.

Recently **Lee and Garimella [11]** investigated heat transfer in microchannels made of copper for Reynolds number 300 to 3500. Width of studied channels ranged from 194 to 534 μm while the depths were five times the widths. In deducing the average Nusselt number, an average wall temperature based on a one-dimensional conduction model was used. For laminar flow the measured Nusselt number agreed with predictions for thermally developing flow over the entire length of the channel. They found that a classical macro scale analysis can be applied to microchannels, although care must be taken to use the proper theoretical or empirical correlation. Many of the empirical correlations available did not match with their experimental data. However, their numerical analysis showed good agreement with their experimental results in the laminar regime. They indicated that considerations of entrance regions and turbulent transitions must be accounted for.

Choi et al. [12] also suggested from their experiments with microchannels that the Nusselt number did in fact depend on the Reynolds number in laminar microchannel flow. They also found that the turbulent regime Nusselt numbers were higher than expected from the Dittus- Boelter equation. **Rahman and Gui [13, 14]** found Nusselt numbers to be high in the laminar regime and low in the turbulent regime.

Adams et al. [15] tested investigated the turbulent single phase forced convective heat transfer when water flow in circular microchannels of hydraulic diameter of 760 μm and 1090 μm. The measured values of Nusselt number were significantly higher than the predicted by conventional correlations. Further deviation in the value of Nusselt number from the convention prediction increased with the increased Re and with decreasing the channel diameter.

The single phase forced convective heat transfer and flow characteristics of water in micro channel structures/plates with small rectangular channel hydraulic diameters of 0.133-0.367 mm and distinct geometric configurations were investigated experimentally by **Peng and Peterson [16]**. The laminar heat transfer was found to be dependent upon the aspect ratio and the ratio of hydraulic diameter to the center-center distance microchannel. The flow resistance of the liquid flow in the microstructures was also investigated experimentally and analytically, and correlations were proposed for the calculation of the flow resistance.

Mokrani et al. [17] developed a reliable experimental device and adequate methodology to characterize the flow and convective heat transfer in flat micro channels. The study was concerned with measurement of pressure drop and heat transfer by a Newtonian fluid flow inside a flat micro channel of rectangular cross

section whose aspect ratio is sufficiently high that the flow can be considered two dimensional They considered the hydraulic diameter as twice of the channel height. The mathematical model used to describe the convective heat transfer between the walls and the fluid takes into account the whole field (solid wall and fluid layer) and the coupling between the conduction and the convection modes. Finally they concluded that the conventional laws and correlations describing the flow and convective heat transfer in ducts of large dimension are directly applicable to the micro channels of heights between 500 and 50 microns.

Mahalingam and Andrews [18] investigated a high-performance air cooling technique for electronic devices and packages that involved high-velocity air flow through micro-structured compact heat sinks of large surface area. The heat transfer calculations performed for the air-cooled narrow channels were described in detail. The channels considered were 0.13 to 0.25 mm wide with an aspect ratio of 10, resulting in heat transfer surface areas of 47 to 63 cm^2 per m^3 of heat sink volume. Experiments and predictions showed that these heat sinks were an attractive alternative to conventional forced air circulation heat sinks in terms of improved electrical performance.

Yu et al. [19] reported experimental investigations on an air-cooled microchannel heat sink. The microchannels considered were of large aspect ratio (62.5) with the expectation that the pressure drop would be lower. The experimentally determined total thermal resistance was found to be in good agreement with that determined from a thermal resistance model, with the assumption of a Nusselt number of 6.5 in the model. The pressure drop was found to have a large discrepancy, up to 18%, from the predicted values, especially at high air flow rates; this was attributed to the entrance and exit losses in the heat sink which were ignored in the pressure

drop calculations. The cooling capacity of the heat sink was approximately 1700 W with a heat flux of approximately 15 W/cm^2 . With a volumetric flow rate of 140 m^3/hr, the pressure drop encountered was found to be as low as 400 Pa.

Aranyosi et al. [20] reported a parametric analysis and experiments on compact heat sinks for power packages, which utilized air impingement cooling in microchannels. A thermal resistance model was developed and used to determine the influence of the operational (static pressure and pumping power) and geometric parameters on thermal resistance. Measured thermal resistances and pressure drops agreed with model predictions to within 20%.

2.4 Numerical Study of Fluid Flow and Heat Transfer in Microchannels

C. J. Crocker, H. M. Soliman, S. J. Ormiston [21], investigated the effect of various geometric parameters, material properties and Re on the thermal performance of the heat sink. They also made comparison between circular and rectangular microchannel at the same Re and hydraulic diameter and showed that sinks with rectangular channel have lower thermal resistance while sinks with circular microchannel dissipate more heat per unit pumping power. Numerical solution of the above was using finite control volume method together with finite element approach.

Reiyu Chein and Janghwa Chen [22], conducted the numerical study of inlet and outlet arrangement effect on microchannel heat sink performance. Because of difference in inlet and outlet arrangement, other remaining same, resultant flow field and temperature distribution are different for a given pressure drop. Using average velocity and fluid temperature in each channel, it was found that better

uniformity in velocity and temperature can be found in the heat sink having cooling supply and collection vertically.

H. Ghaedamini, P.S. Lee , C.J. Teo [23], studied the effect of geometric configuration on the heat transfer performance and fluid flow of converging-diverging microchannel numerically. For five different aspect ratios and wall curvature, Nu and *f* were defined for three different Re 200, 400 and 600. For the regular advection region, increasing in waviness will result in better heat transfer performance as long as two counter rotating vortices are not present in trough region. For chaotic advection, heat transfer rate increases with higher pressure drop.

2.5 Closure

The literature review above reveals the fact that numerical simulation i.e; CFD analysis of experimental work done by **Adams et al.** i.e forced convective heat transfer with turbulent flow through circular microchannel of diameter 0.76 mm subjected to uniform heat flux of 3000 W/m^2, has not been undertaken and validated. Moreover sinks with circular microchannel dissipate more heat per unit pumping power when compared to rectangular microchannel [2]. This is the main motivation behind the present work.

Finally the experimental investigation results are practically needed results because experimental results are required to validate the CFD codes. In this study the governing equations has been solved by SIMPLE method and analyzed the results obtained.

2.6 Objective of the Present Work

There has been limited number of research work on the performance of microchannel heat sink using CFD model. Therefore, the objective of the present work is

- To do the simulation of a circular microchannel of diameter 0.76mm and 1.09mm using water as a coolant, the central part of which is subjected to uniform heat flux.
- To compare the simulation of microchannel when using water and air as coolant.
- To show the variation of temperature, velocity, pressure etc. along the centerline of the pipe.
- To show the variation of wall shear along the pipe wall.
- To calculate the Nusselt in the heated region of the pipe.
- To compare axial velocity and temperature variation at different locations.
- To show velocity vector, pressure, temperature and pressure contour in the entire flow regime.
- To show the variation in wall temperature of the microchannel.
- To validate the CFD simulation.

3. MATHEMATICAL FORMULATION

3.1 Introduction

A two dimensional analysis of single phase flow and heat transfer has been carried in a circular microchannel of diameter 0.76 mm and of length 152.4 mm. Initial length of 63.5 mm which is insulated, precedes the heated section. This ensures that the flow is fully developed before entering the heated region. The heated length of microchannel is subjected to uniform heat flux intensity of 3000 W/m^2. After the heated region insulated microchannel of length 152.4 mm follows. Distilled water has been used as the coolant which is entering inlet of the microchannel with velocity of u = 18 m/s. the operating pressure is 1 atm in absolute scale. A schematic diagram of the problem has been shown in the figure below.

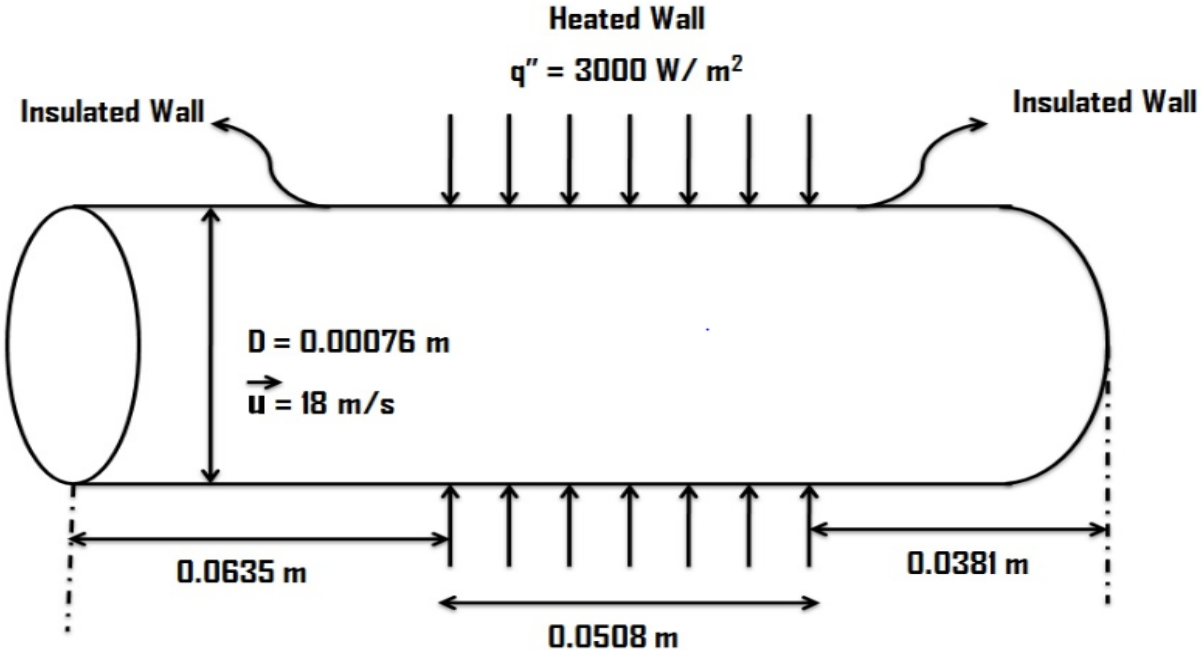

Fig. 3.1 Fluid flow through a circular micro channel

3.2 CFD Modelling

3.2.1 Introduction

Computational fluid dynamics (CFD) is a computer based numerical tool which is used for analyzing flow of fluid, its heat transfer characteristics and to study other parameters related to fluid flow and heat transfer. It imposes different equations such as continuity, momemtum and energy equations etc. on the elementary cells generated by meshing. Conservation laws are in the form of partial differential equations. These equations are solved using FLUENT software. FLUENT is a finite volume program with the help of which geometry is generated and meshing is done. Thus fluid flow and heat transfer problems are solved with the help of FLUENT. The solution converges after certain number of iterations and thereafter in the post processor different results are shown, contours and graphs are plotted.

3.2.2 Advantages of Using CFD Modeling

- It gives us better understanding of fluid flow heat transfer characteristics or other parameters.
- CFD modeling helps in minimizing chances of errors.
- Once the result obtained by CFD gets validated, change in design, boundary conditions along with results can easily be accompanied.
- It is a cost effective method as experimental set up for every different design and conducting the experiment is costly.
- It saves time for studying flow parameters and analyzing results.

3.2.3 Governing Equations:

In axis symmetric geometry continuity equation gets transformed as

$$\frac{\partial \rho}{\partial t} + \frac{\partial}{\partial x}(\rho \upsilon_x) + \frac{\partial}{\partial r}(\rho \upsilon_r) + \frac{\rho \upsilon_r}{r} = 0 \quad \text{... (1)}$$

Where, x is axial direction while r is radial direction.

In case of 2D axis symmetric problem the momentum conservation equation in axial and radial direction is given as below:

$$\frac{\partial}{\partial t}(\rho v_x) + \frac{1}{r}\frac{\partial}{\partial x}(r\rho v_x v_x) + \frac{1}{r}\frac{\partial}{\partial r}(r\rho v_r v_x) = -\frac{\partial p}{\partial x} + \frac{1}{r}\frac{\partial}{\partial x}\left[r\mu\left(2\frac{\partial v_x}{\partial x} - \frac{2}{3}(\nabla.\vec{v})\right)\right] + \frac{1}{r}\frac{\partial}{\partial r}\left[r\mu\left(\frac{\partial v_x}{\partial r} + \frac{\partial v_r}{dv_x}\right)\right] + F_x \quad \ldots\ldots\ldots (2)$$

And

$$\frac{\partial}{\partial t}(\rho v_r) + \frac{1}{r}\frac{\partial}{\partial x}(r v_x v_r) + \frac{1}{r}\frac{\partial}{\partial r}(r v_r v_r) = -\frac{\partial p}{\partial r} + \frac{1}{r}\frac{\partial}{\partial x}\left[r\mu\left(\frac{\partial v_r}{\partial x} + \frac{\partial v_x}{\partial r}\right)\right] + \frac{1}{r}\frac{\partial}{\partial r}\left[r\mu\left(2\frac{\partial v_r}{\partial r} - \frac{2}{3}(\nabla.\vec{v})\right)\right] - 2\mu\frac{v_r}{r^2} + \frac{2}{3}\frac{\mu}{r}(\nabla.\vec{v}) + \rho\frac{v_z^2}{r} + F_r \quad \ldots\ldots\ldots (3)$$

Where

$$\nabla.\vec{v} = \frac{\partial v_x}{\partial x} + \frac{\partial v_r}{\partial r} + \frac{v_r}{r} \quad \ldots\ldots\ldots (4)$$

Since the microchannel thickness is small and it is horizontally placed, body forces Fx and Fr is taken to be zero. This will modify eqn. 2 and eqn. 3 as below:

$$\frac{\partial}{\partial t}(\rho v_x) + \frac{1}{r}\frac{\partial}{\partial x}(r\rho v_x v_x) + \frac{1}{r}\frac{\partial}{\partial r}(r\rho v_r v_x) = -\frac{\partial p}{\partial x} + \frac{1}{r}\frac{\partial}{\partial x}\left[r\mu\left(2\frac{\partial v_x}{\partial x} - \frac{2}{3}(\nabla.\vec{v})\right)\right] + \frac{1}{r}\frac{\partial}{\partial r}\left[r\mu\left(\frac{\partial v_x}{\partial r} + \frac{\partial v_r}{dv_x}\right)\right] \quad \ldots\ldots\ldots (5)$$

And

$$\frac{\partial}{\partial t}(\rho v_r)+\frac{1}{r}\frac{\partial}{\partial x}(r v_x v_r)+\frac{1}{r}\frac{\partial}{\partial r}(r v_r v_r)=-\frac{\partial p}{\partial r}+\frac{1}{r}\frac{\partial}{\partial x}\left[r\mu\left(\frac{\partial v_r}{\partial x}+\frac{\partial v_x}{\partial r}\right)\right]$$
$$+\frac{1}{r}\frac{\partial}{\partial r}\left[r\mu\left(2\frac{\partial v_r}{\partial r}-\frac{2}{3}(\nabla.\vec{v})\right)\right]-2\mu\frac{v_r}{r^2}+\frac{2}{3}\frac{\mu}{r}(\nabla.\vec{v})+\rho\frac{v_z^2}{r}$$

..... (6)

In the present problem standard *k-ε* model has been selected as the flow is turbulent. Transport equations that are used by ANSYS for single phase turbulent flow are as follows:

$$\frac{\partial}{\partial t}(\rho k)+\frac{\partial}{\partial x_i}(\rho k v_i)=\frac{\partial}{\partial x_j}\left[\left(\mu+\frac{\mu_t}{\sigma_k}\right)\frac{\partial k}{\partial x_j}\right]+G_k+G_b-\rho\varepsilon-Y_M+S_k$$

..... (7)

And

$$\frac{\partial}{\partial t}(\rho\varepsilon)+\frac{\partial}{\partial x_i}(\rho\varepsilon v_i)=\frac{\partial}{\partial x_j}\left[\left(\mu+\frac{\mu_t}{\sigma_\varepsilon}\right)\frac{\partial \varepsilon}{\partial x_j}\right]+C_{1\varepsilon}\frac{\varepsilon}{k}(G_k+C_{3\varepsilon}G_b)-C_{2\varepsilon}\rho\frac{\varepsilon^2}{k}+S_\varepsilon$$

...(8)

3.3 Geometry in ANSYS Workbench

As per our problem specification cross-section of microchannel is circular and heat flux is uniform, the flow is assumed to be axis symmetric. When we opt for axis symmetric Cartesian coordinates gets converted into cylindrical polar coordinates. It implies that flow parameters vary in axial direction corresponding to x coordinate and radial direction corresponding to y coordinates in 2-D geometry. The properties are assumed to be independent of azimuthal coordinate θ.

Therefore the above problem microchannel can be modeled in rectangular domain.

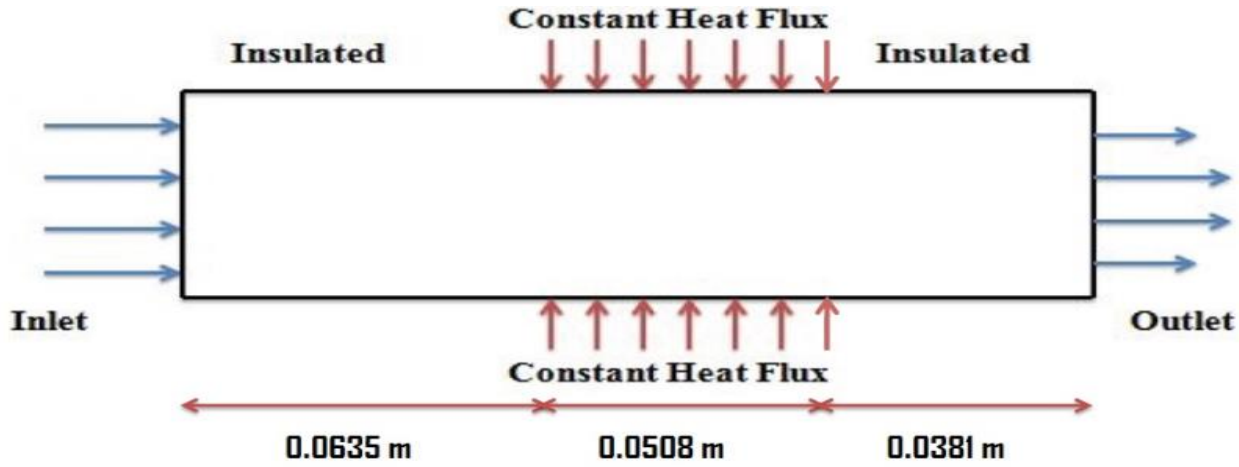

Fig. 3.2 Schematic diag. of circular microchannel as per problem specification

In ANSYS workbench it will appear as below:

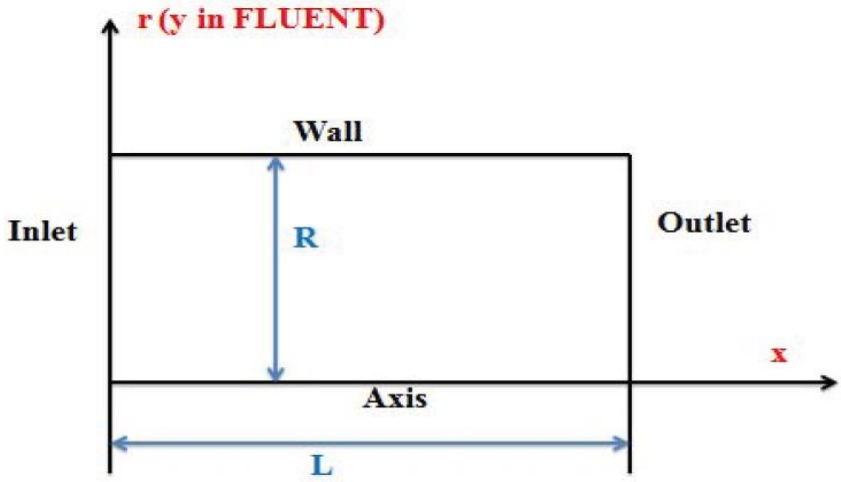

Fig 3.3 2D geometry in ANSYS workbench

R= radius of microchannel

L= length of microchannel

When we rotate the above geometry 360 degrees about the axis of the channel, the entire geometry of channel is recovered.

From analysis system of ANSYS, FLUENT is launched. After FLUENT is launched we go to the properties of geometry. In advance geometry option we

change the analysis type to 2D from 3D which is by default the analysis type in ANSYS 14.5. When the type of analysis is changed to 2D the graphics window of ANSYS appears as below:

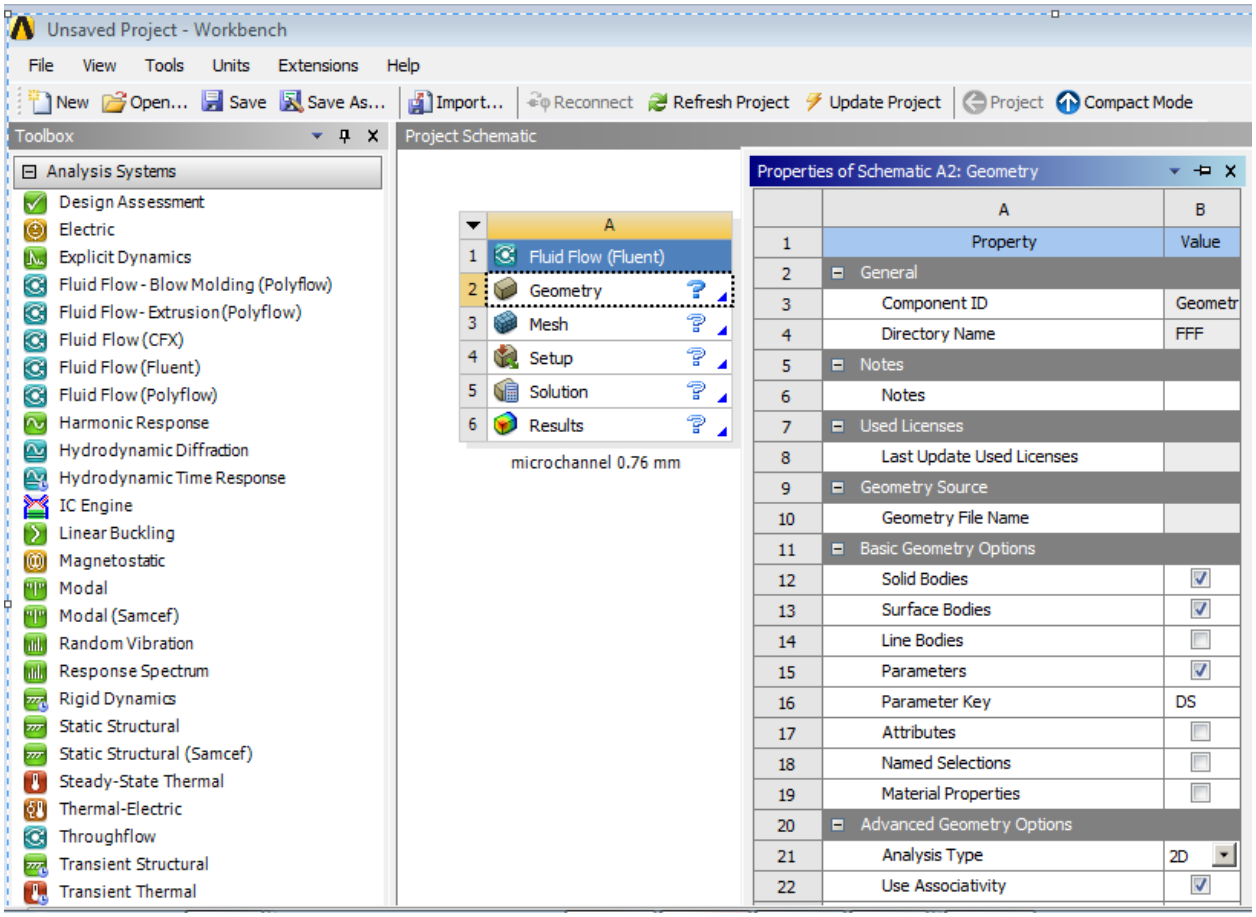

Fig. 3.4 changing analysis type from 3D to 2D

Now Design Modeler is launched and meter is set as default unit. In the present case geometry is a rectangle of length 0.1524m and 0.00038m height. First of all XY plane is chosen for the geometry. From sketching tool box rectangle is selected. Bt the present problem demands three separate section of the channel namely two insulated and one heated region. For that purpose the geometry is modified and drawn rectangle is split into three parts and thereafter top and bottom

edges of splitted portion is set to be equal by subjecting the splitted portion to the constraint of equal length.

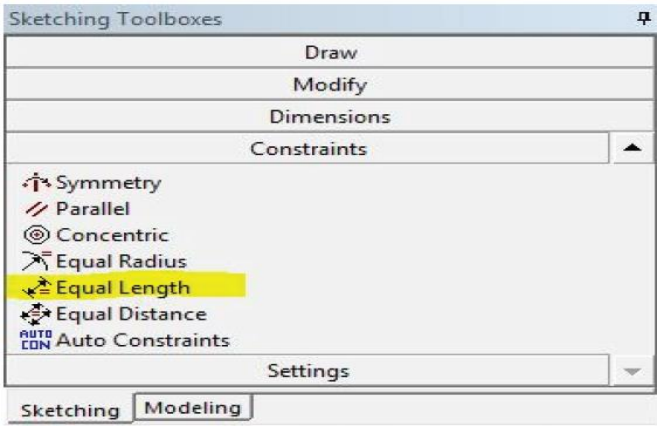

Fig. 3.5 splitting the edge of rectangle into three section

Now dimensioning is done. In the present problem there are three horizontal edges and one vertical edge. They are dimensioned as H1 = 0.0635m, H2 = 0.0508m, H3 = 0.0381m and V1 = 0.00038m. As the analysis type is 2D, surface body is created from the sketch by clicking on any edge of the sketch and applying the base objects.

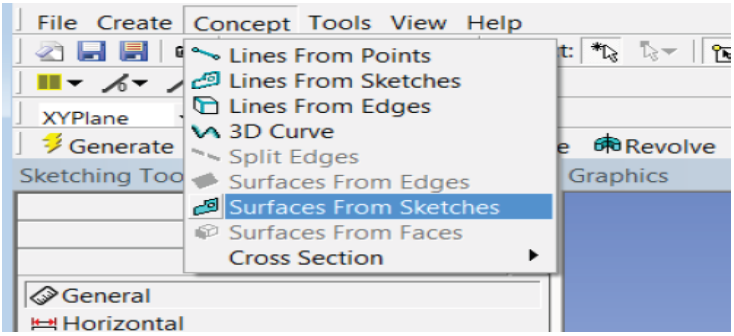

Fig 3.6 creation of surface body from sketch

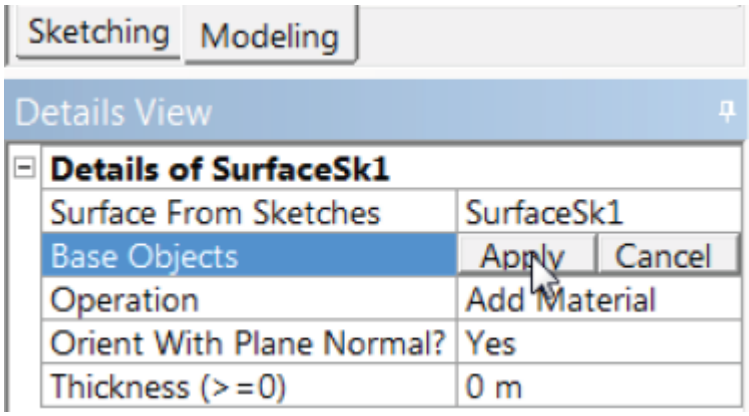

Fig 3.7 creation of geometry from the drawn rectangle

The generated geometry appears as below:

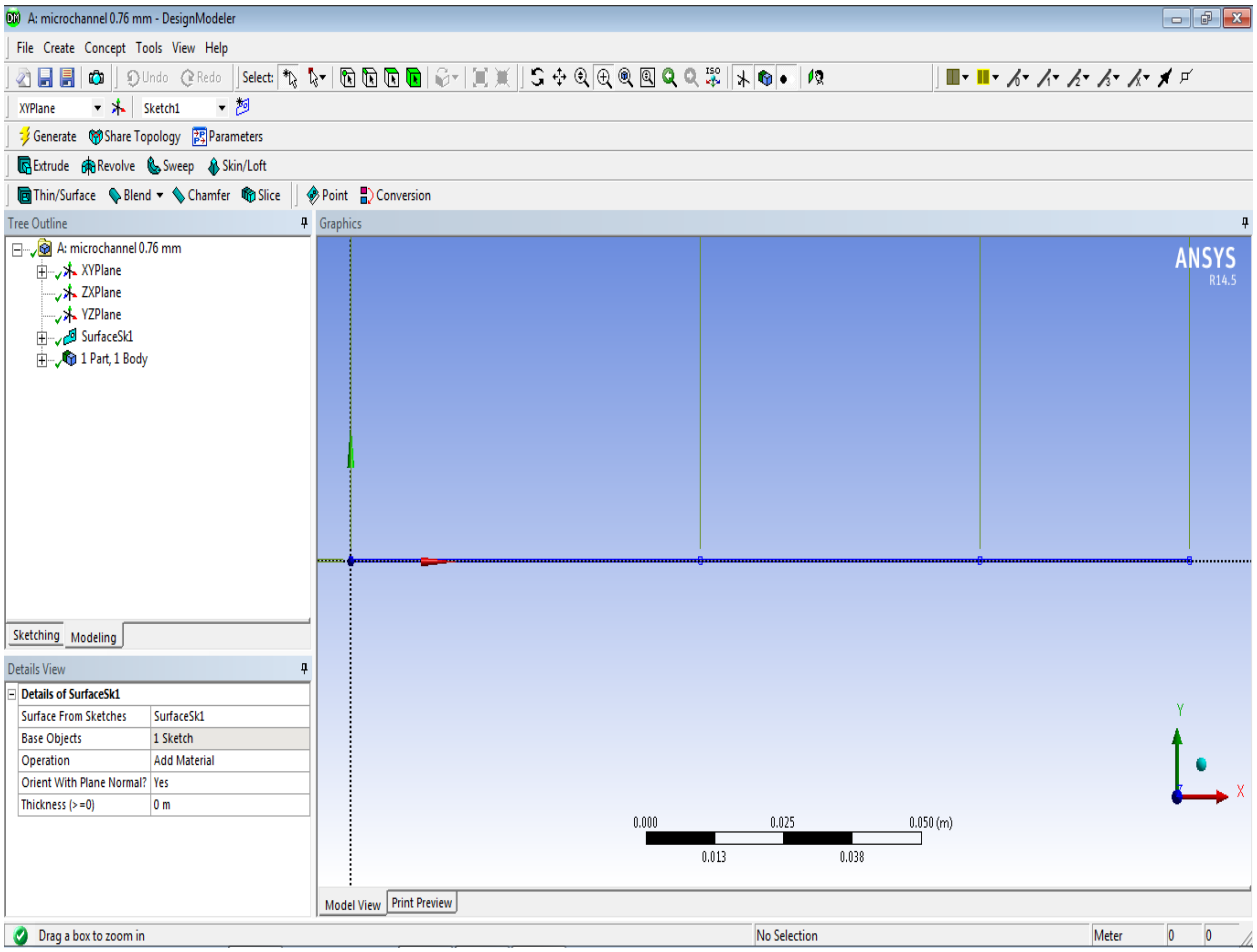

Fig. 3.8 2D geometry of circular microchannel generated by FLUENT

3.4 Meshing of Geometry

Fluent mesher is launched and advanced size function is turned off. Mapped Face Meshing is selected as meshing method.

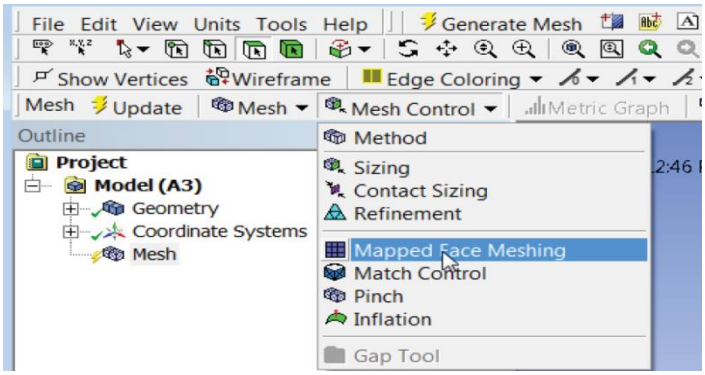

Fig. 3.9 Mapped Face Meshing

Mesh size is controlled by providing element size to horizontal edges of the rectangle and number of divisions to the vertical edges. In the present work element size has been specified to be 8.82 × 10^ (- 4).

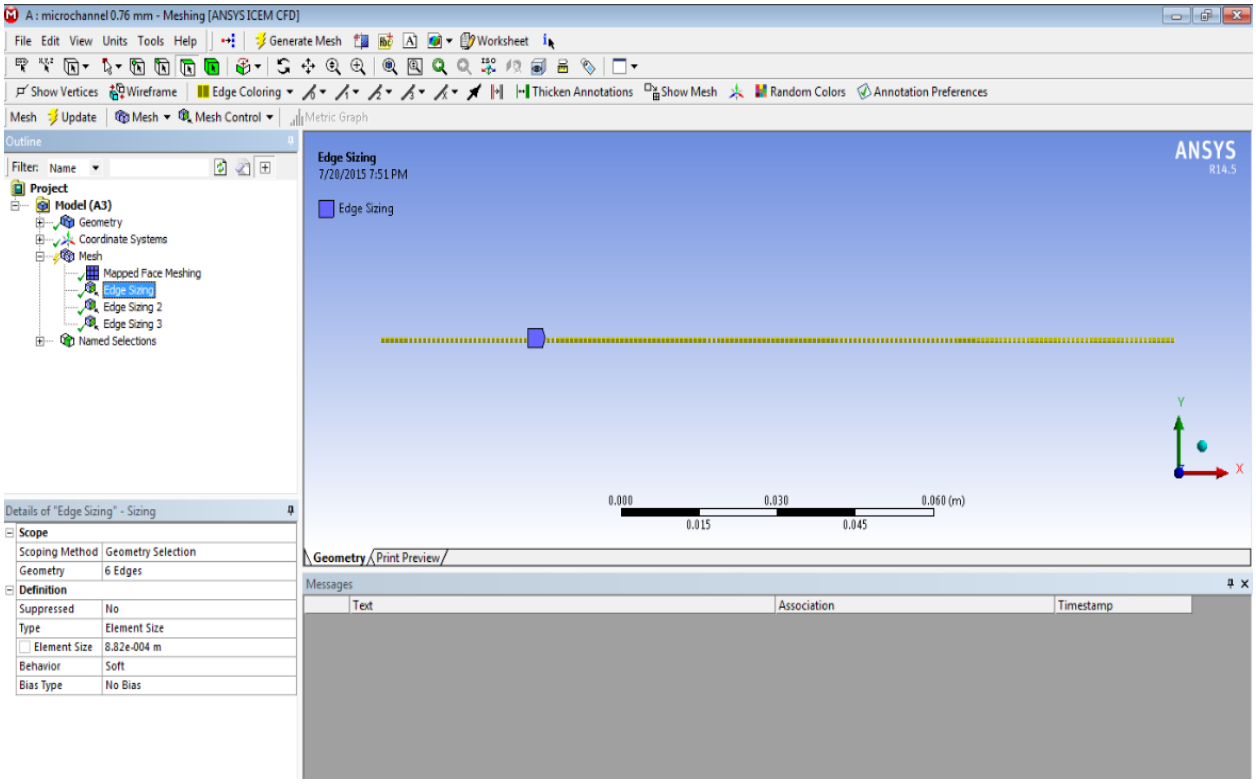

Fig. 3.10 sizing horizontal edges

Now sizing of edge corresponding to inlet is done. It corresponds to edge sizing 2. In the present problem the sizing type of inlet has been set as number of divisions which is 30 and behavior is hard while 10 has been provided as bias factor.

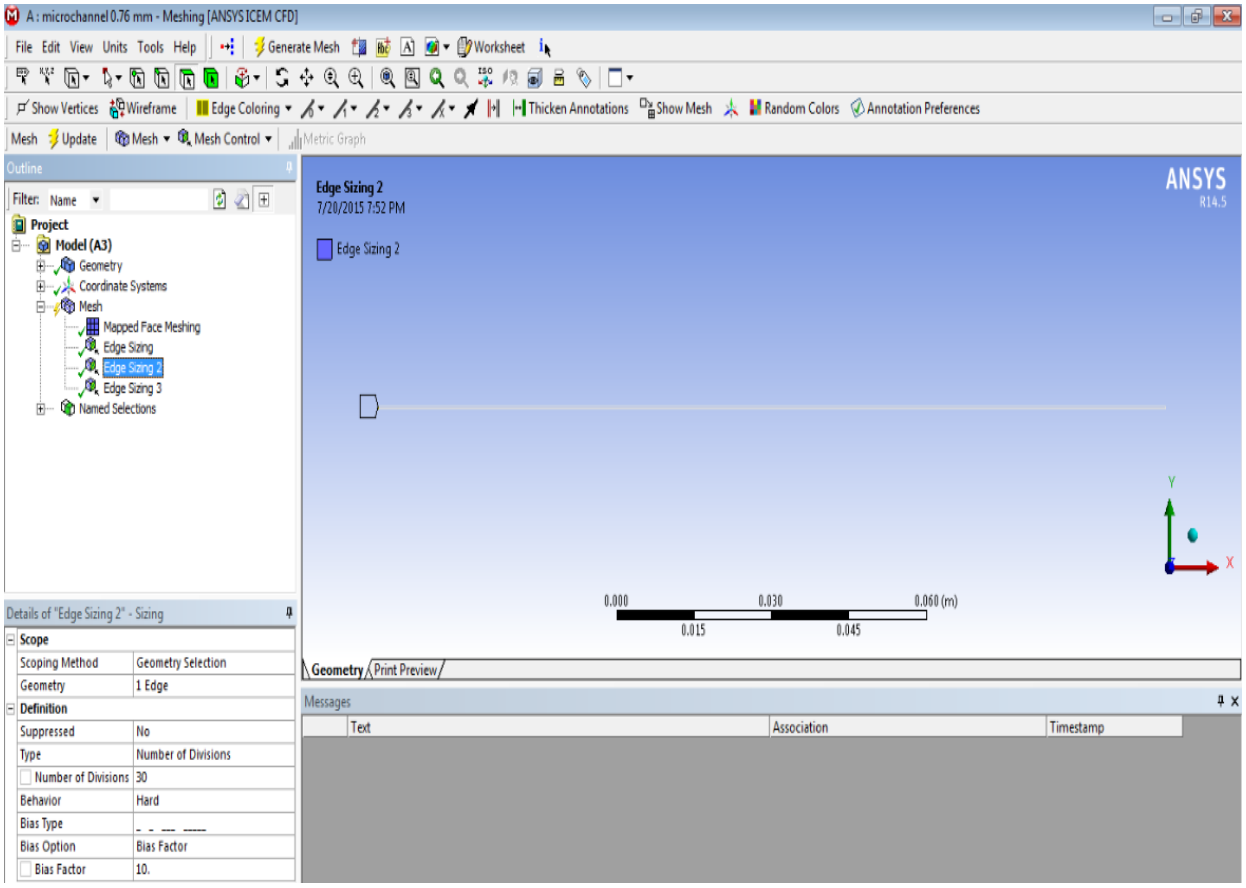

Fig. 3.11 edge sizing 2 corresponding to inlet

Now edge sizing of outlet is done in the similar manner as that of inlet i.e sizing type was set up as no of divisions which is 30 in this case also. Behavior is hard and 10 has been specified as bias factor. The only difference being the type of bias is selected as 1st one while for the inlet it was 2nd.

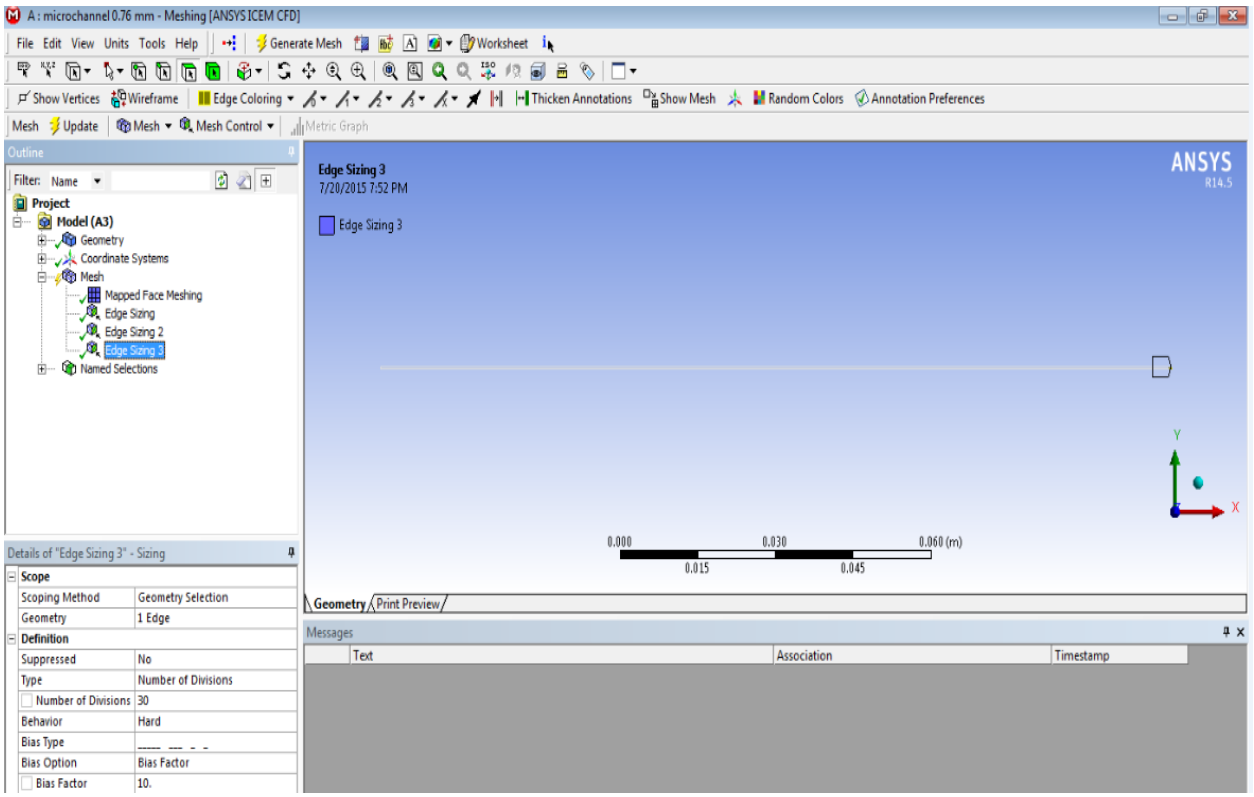

fig. 3.12 edge sizing 3 corresponding to outlet

After providing these inputs mesh is generated that appears as below:

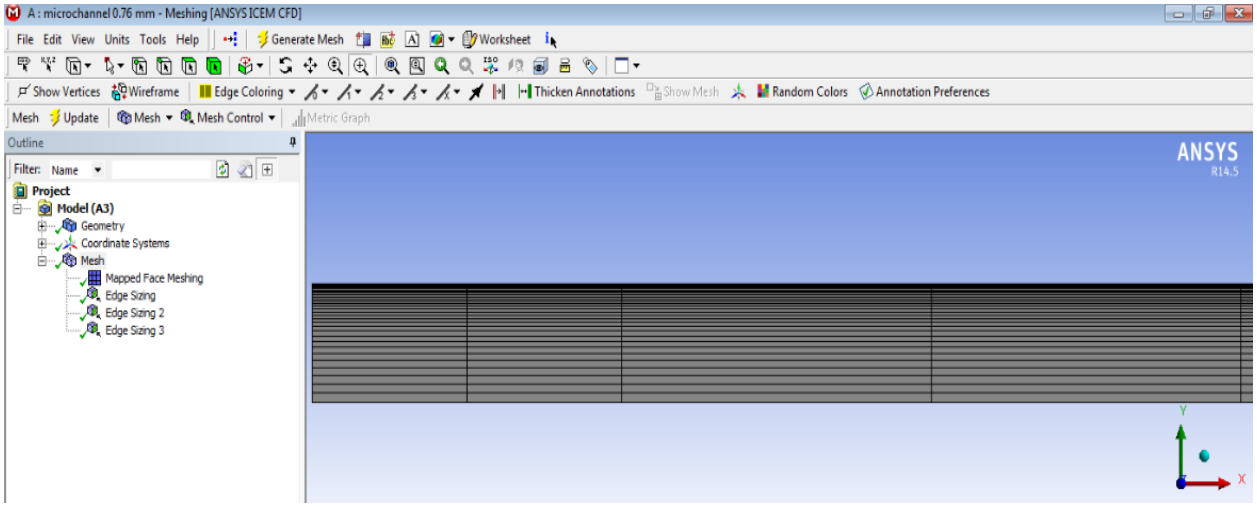

Fig 3.13 mesh generated by FLUENT

The generated mesh is finer near the channel wall which facilitates accurate calculation of flow property near the channel wall.

3.4.1 Creation of Named Section

Edges are named so that proper specification of boundary condition may be possible. Edges are named as inlet, outlet, centerline, wall, heated wall and flow domain.

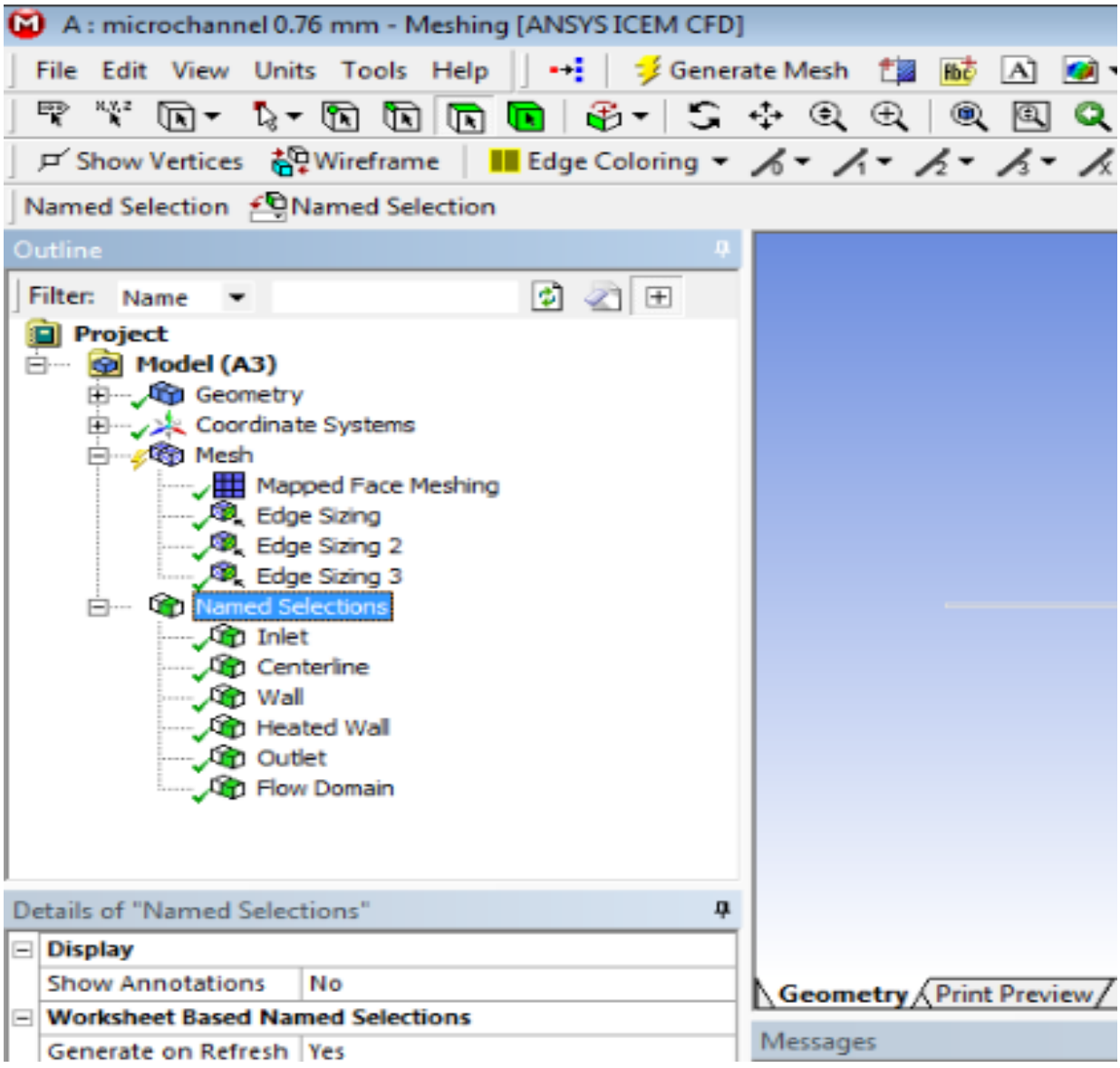

Fig. 3.14 creation of named section

This completes meshing of the geometry generated.

3.5 Physical Setup

Double precision solver is selected for the present problem.

Fig. 3.15 selection of double precision solver

As we select axis symmetric, Cartesian coordinates gets transformed into cylindrical polar coordinates.

$$\nabla = \widehat{e_r}\frac{d}{dr} + \widehat{e_z}\frac{d}{dz} \quad \text{...} \quad (9)$$

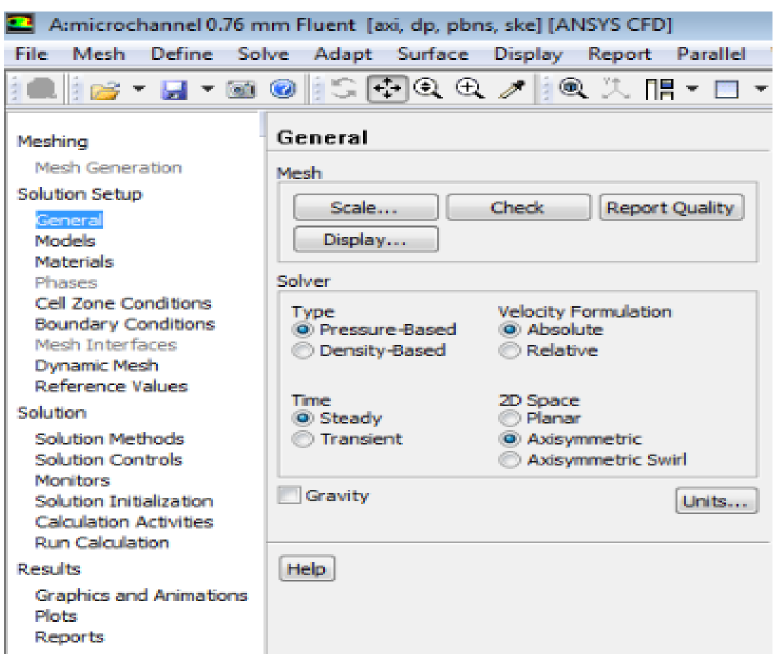

Fig. 3.16 selection of axis symmetry for 2D space in solution setup

3.5.2 Model

While setting up the problem energy equations are turned on, *k-epsilon (2eqn)* is selected for the viscous model and enhanced wall treatment is chosen for the near wall treatment.

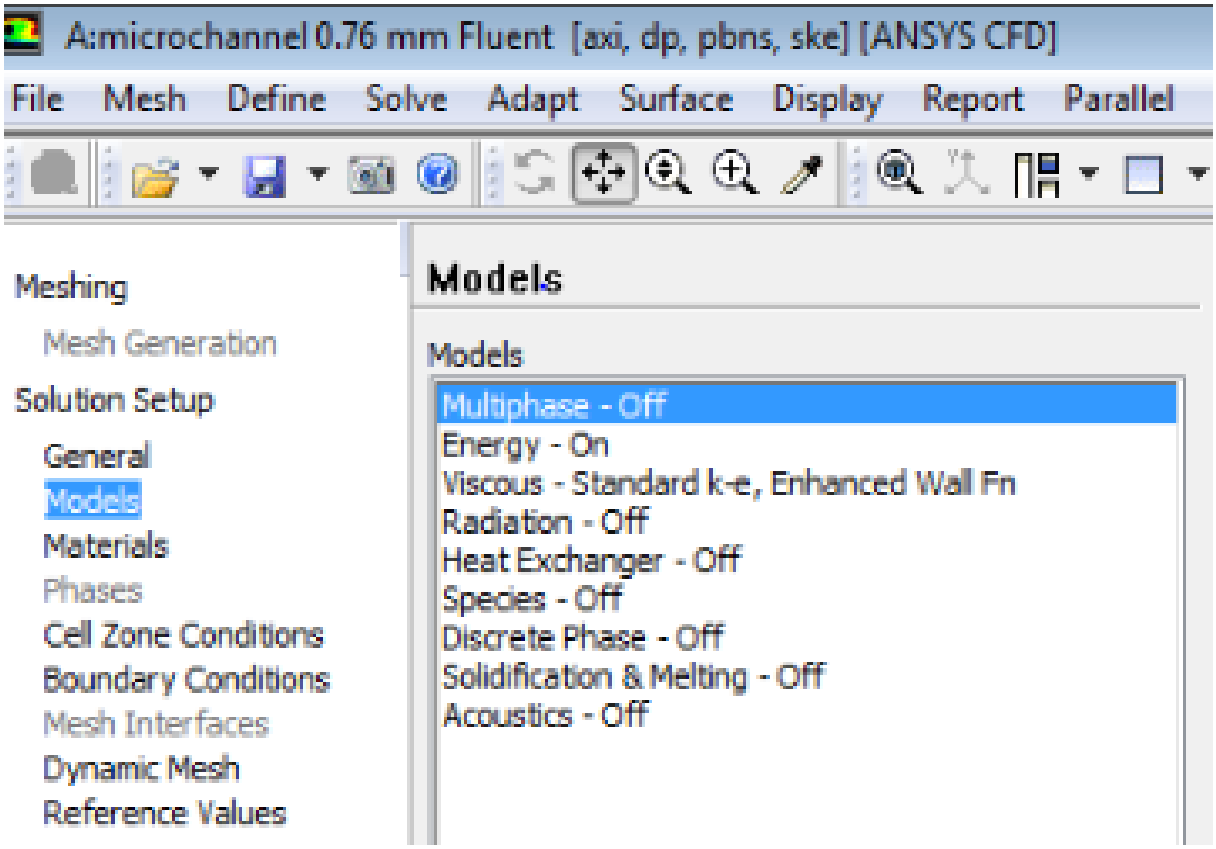

Fig. 3.17 setting up the model of the problem

3.5.3 Material

After the model has been set up, material for fluid and microchannel wall is selected as water and copper respectively. Their properties are used from the fluent database. Air and aluminum is default material for fluid and solid in ANSYS which needs to be edited.

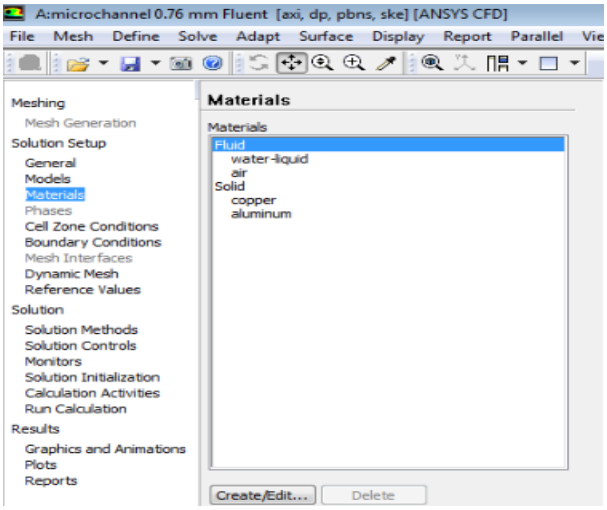

Fig. 3.18 setting up material for fluid and solid

3.5.4 Boundary Conditions

For solving the problem it is essential to define boundary conditions. The operating pressure is set as atmospheric pressure which is 101325 Pa.

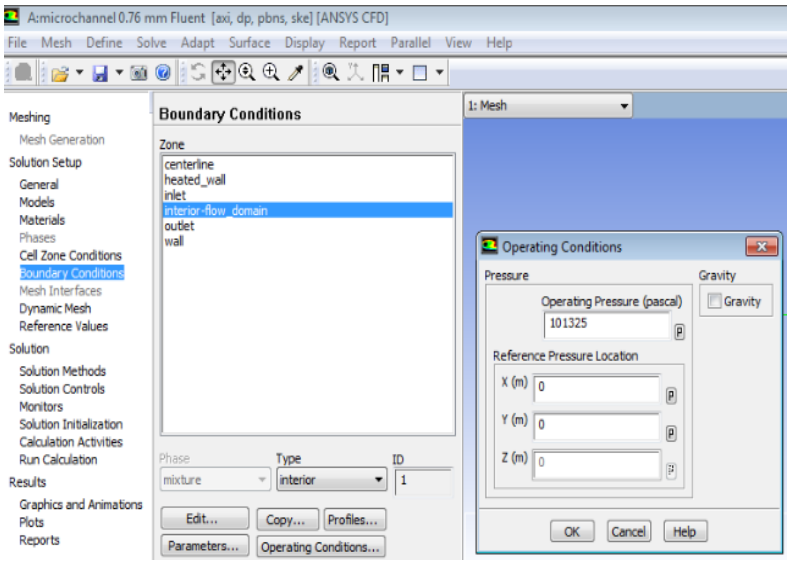

Fig. 3.19 operating conditions

Now boundary condition of centerline is defined and the type of centerline is changed to axis. Gradients at centerline is set up according to assumption i.e; axis symmetry that we made for the centerline.

For heated wall, boundary condition is set up by specifying heat flux to be 3000 W/m^2.

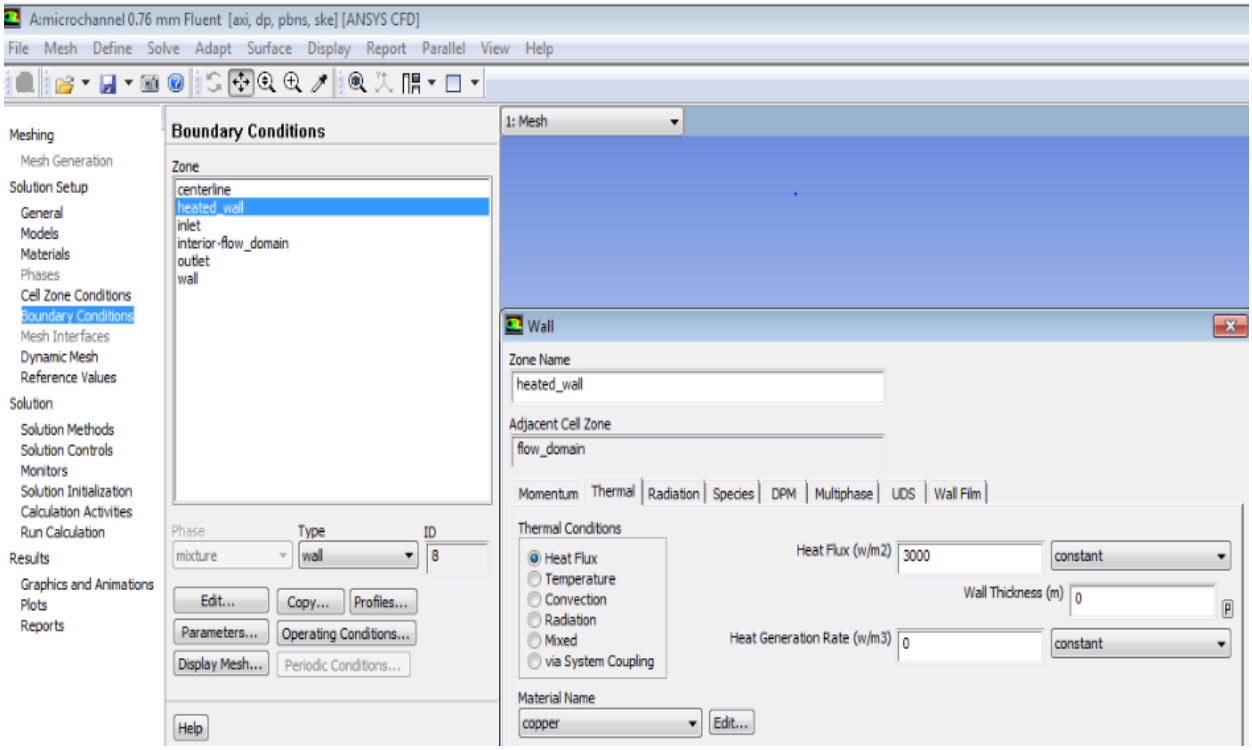

Fig. 3.20 heated wall subjected to uniform heat flux of 3000 W/m^2

Portion other than heated wall is set as insulated wall by subjecting them to zero heat flux.

Boundary condition at the inlet is set to velocity type and specifying axial velocity to be 18 m/s, percentage intensity of turbulence as 5% and turbulent viscosity as ratio as 10.The provided value of percentage intensity of turbulence and turbulent viscosity ratio at the inlet is for the sake of initial guess for the FLUENT to solve *k-ε* equations.

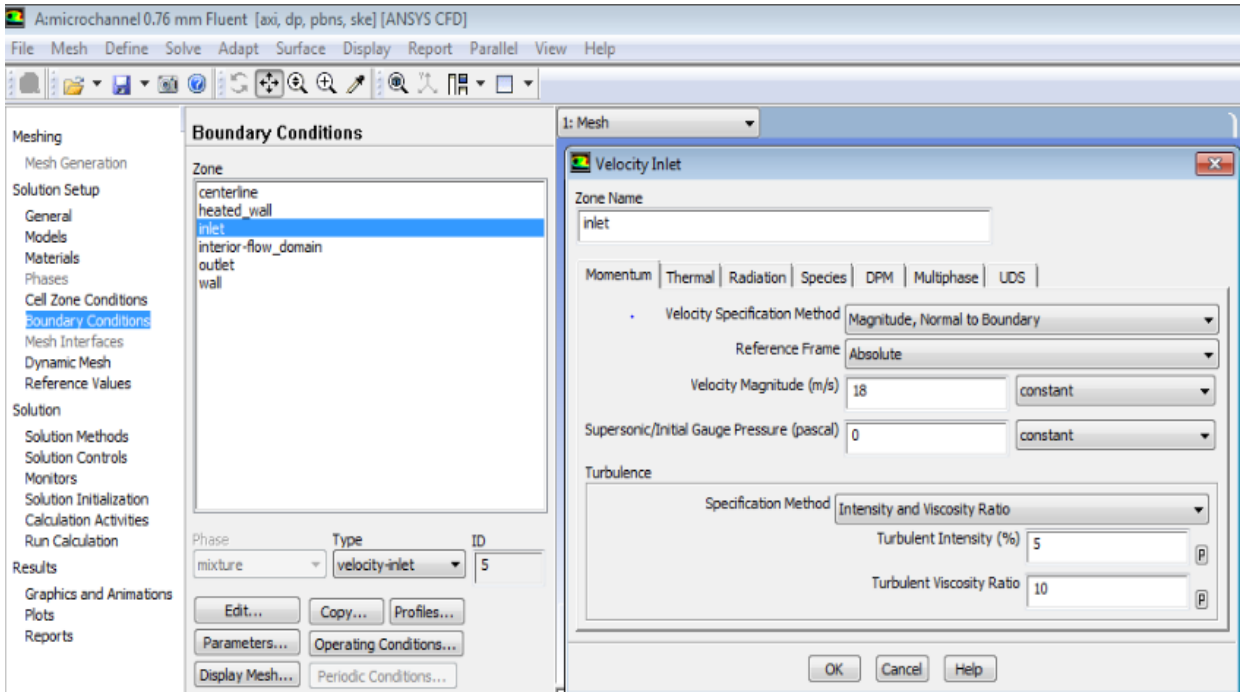

Fig. 3.21 boundary conditions at the inlet of channel

Boundary condition for outlet is set by specifying gauze pressure to be zero, percentage of backflow turbulent intensity as 5% and backflow turbulent viscosity ratio as 10 which is the default value of FLUENT.

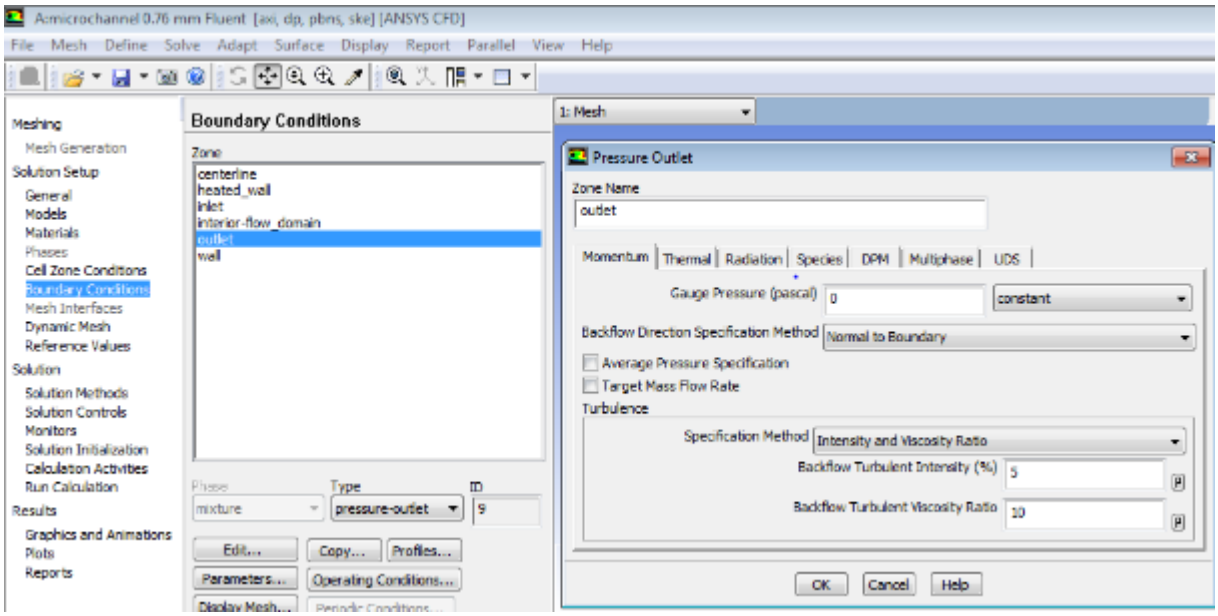

Fig. 3.22 boundary conditions at the outlet of the channel

3.6 Numerical Solutions

Governing equations that FLUENT uses to solve the problem are non-linear equations which are solved in a no of iterations.

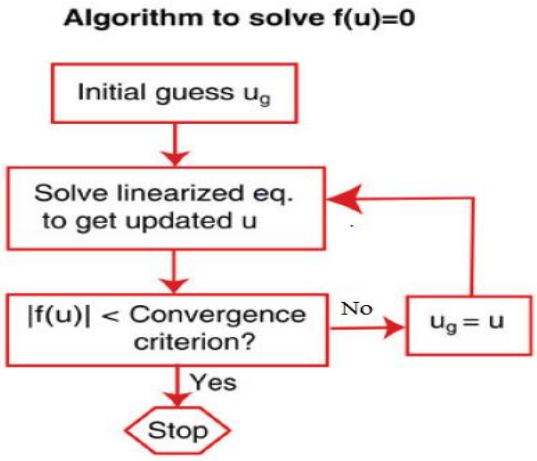

Fig. 3.23 algorithm showing iteration process

In order to start iteration we need to provide initial guess for flow variable and convergence criterion as well. The FLUENT solves our boundary value problem by converting it to a set of algebraic equations. It is done by discretization process. For all equations 2nd order upwind is chosen in order to minimize the error.

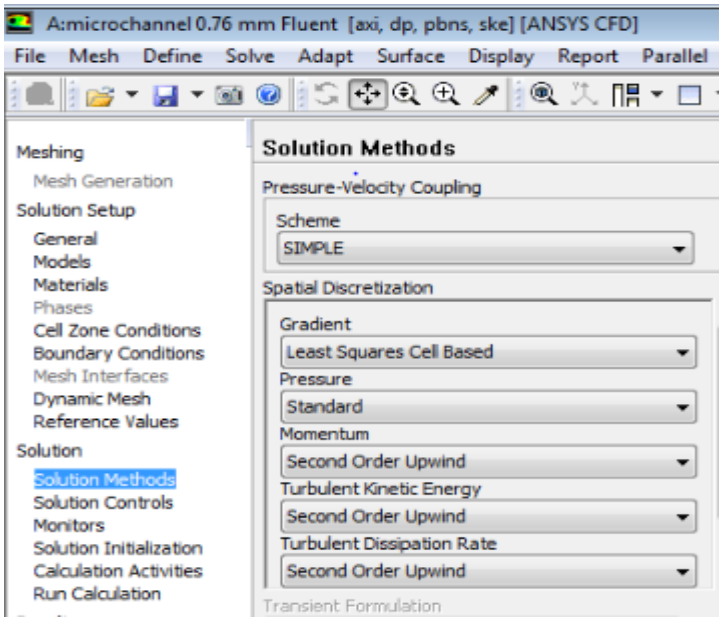

Fig. 3.24 solution methods

Convergence criterion for all differential equations are set as 10^-6. This is accomplished by editing solution controls. Number of iterations is set as 1000.

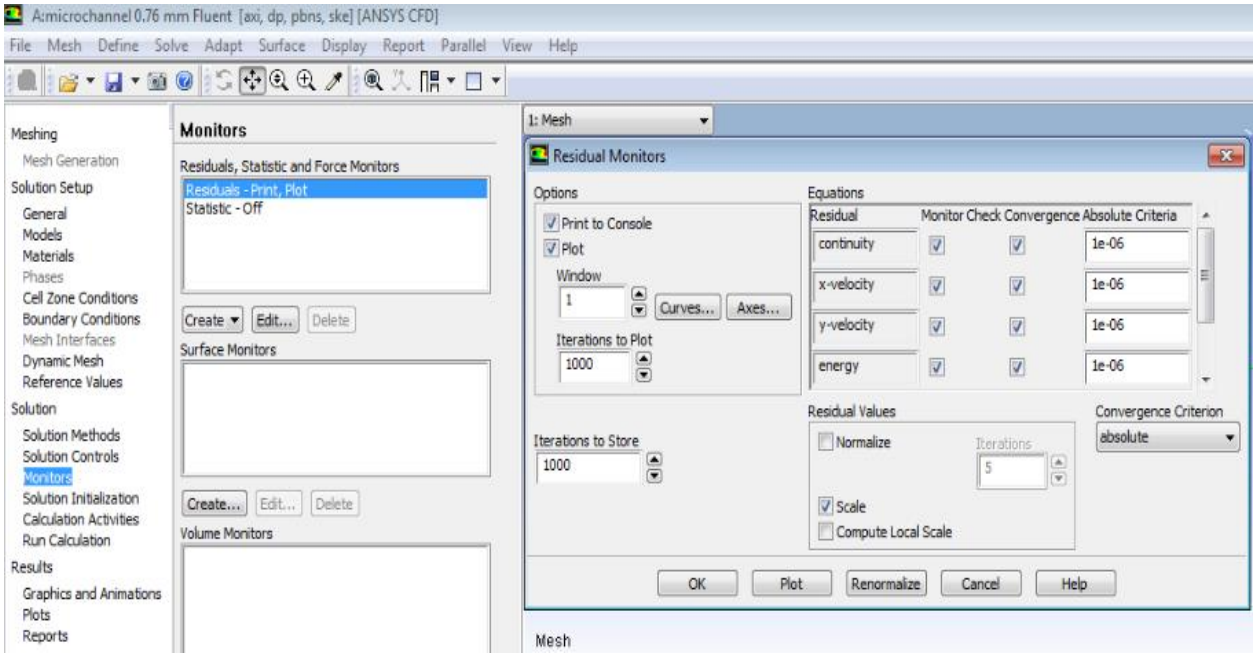

Fig. 3.25 setting the convergence criterion and number of iterations

Standard initialization is selected as the method of solution initialization. Compute from inlet is selected and thereafter solution is initialized.

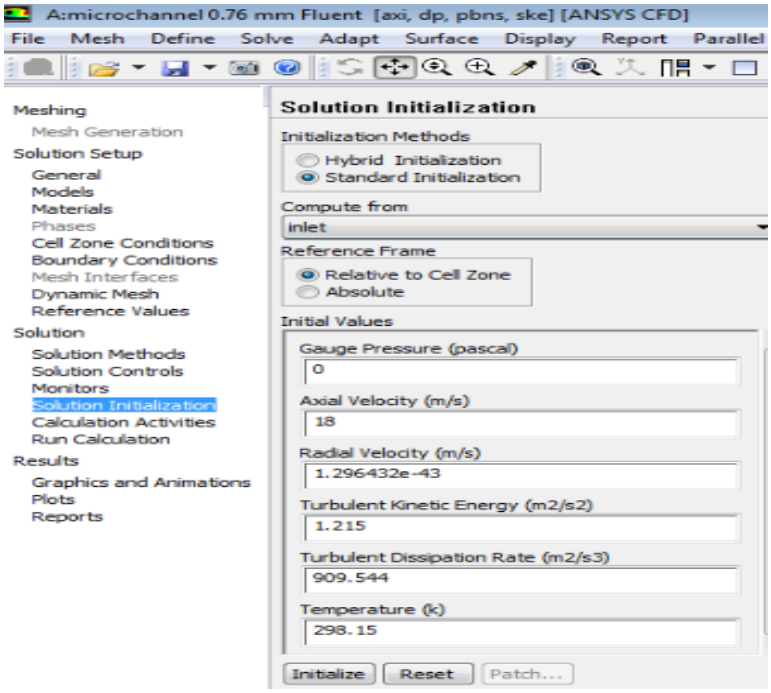

Fig. 3.26 solution initialization

Computer is prevented from iterating indefinitely by putting a limit on the number of iterations as 1000 and thereafter we run the solution. In the present case solution converges in 316 iterations.

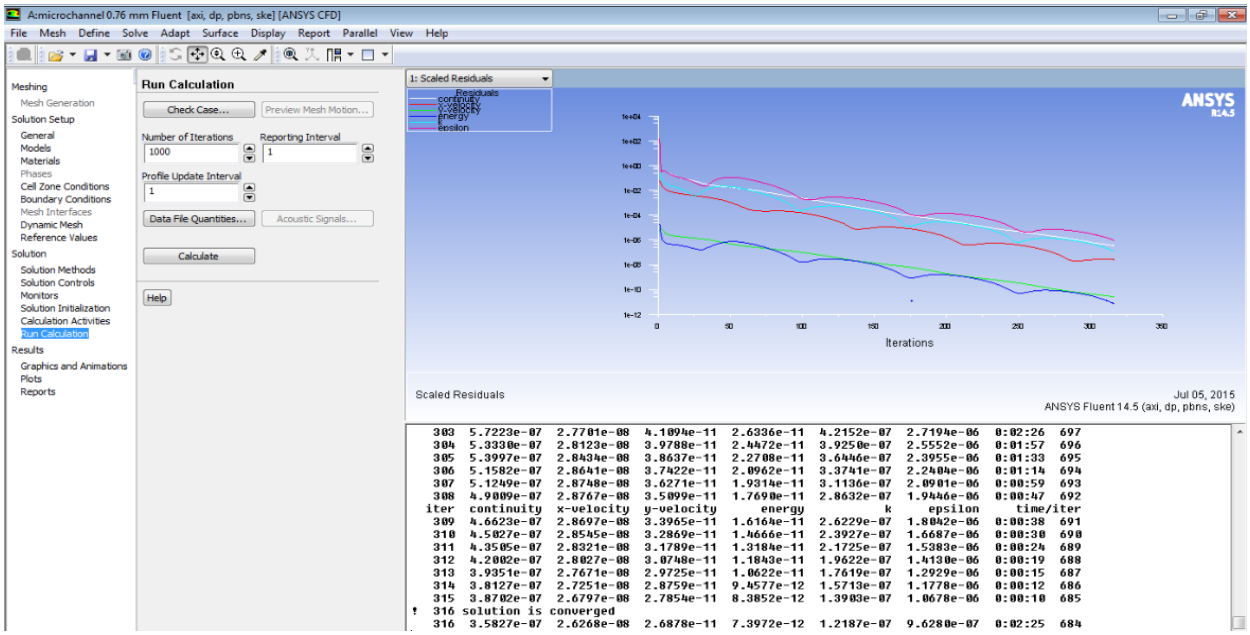

Fig. 3.27 iterations and convergence of solution

If we want to analyze skin friction coefficient other than standard quantities, skin friction coefficient is transferred to post-processor from additional quantities.

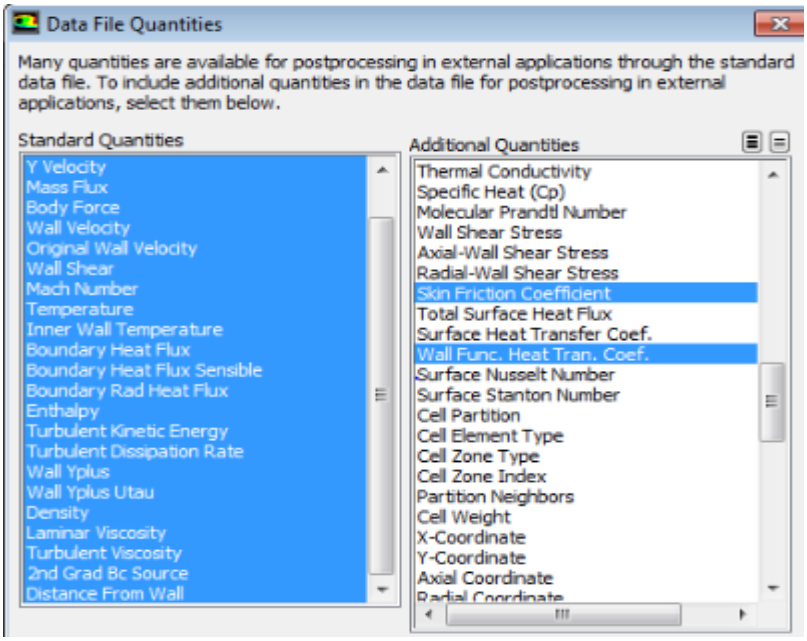

Fig. 3.28 transfer of skin friction coefficient to post processor

4. RESULTS AND DISCUSSIONS

4.1 Introduction

A 2-D model was developed to study and analyze the fluid flow and heat transfer in the circular channel. A number of calculations are performed by FLUENT and results are produced to show the variation of different parameters.

4.2 Simulation of Circular Microchannel

4.2.1 Velocity Vector

For velocity vector location is selected as periodic 1. This facilitates the display of velocity vector periodically along the entire surface of geometry. Line arrow is selected as symbol and symbol size is selected as 0.1. ANSYS 14.5 displays only half of the cross section thereby showing velocity vector and other variation of half of the cross section only. In view tab, mirroring condition is applied about ZX plane in default transform to work out this problem. In order to have a better view of the result, scale is applied and set as (1, 30, 1). This stretches the result in Y direction by 30. After all these settings, velocity vector appears as below:

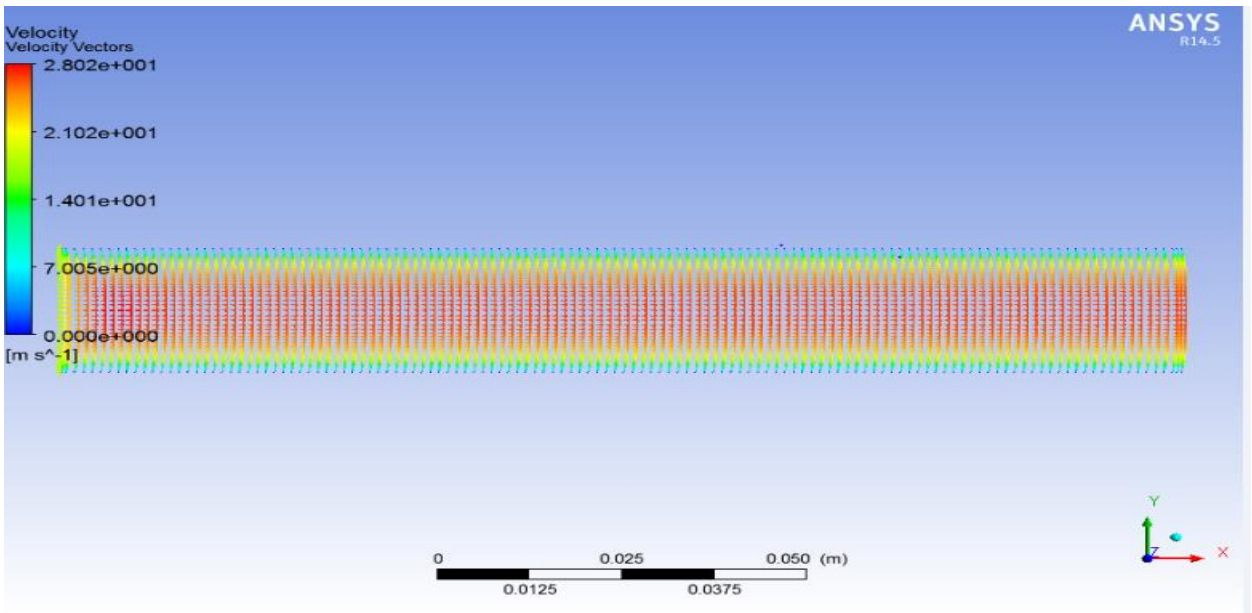

Fig. 4.1 velocity vector

4.2.2 Velocity Contour

For plotting velocity contour, first of all we open the contour tab and in geometry tab periodic 1 is selected as location. Velocity is set as variable and again for viewing option reflection or mirroring is selected. Method of mirroring is selected as zx plane and again we apply scale in order to have better view of result which is set as (1, 30, 1). This stretches our result in y direction. After all these settings our velocity contour appears as below:

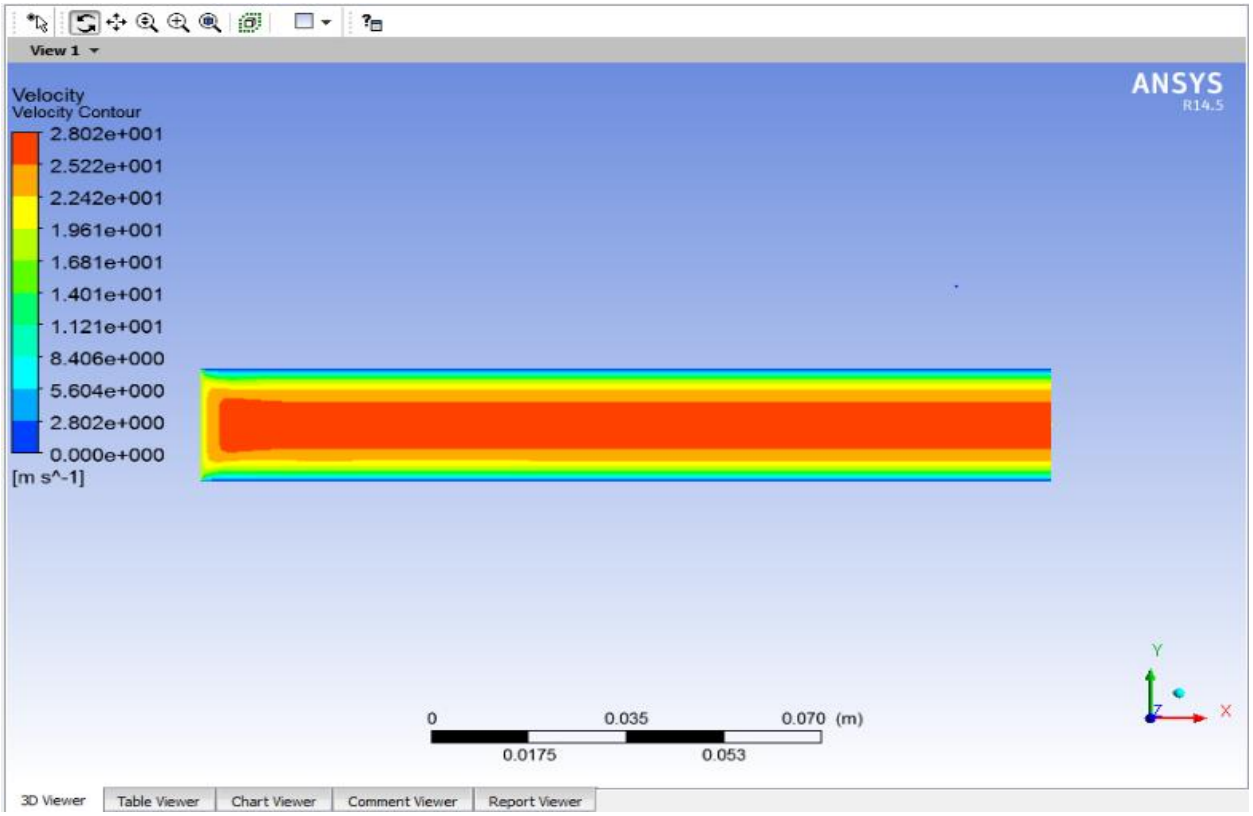

Fig. 4.2 velocity contour

The minimum value of velocity is zero which is near the wall of the channel which is in no slip condition and the maximum value of velocity is 28.0201 m/s which is in the central region near the axis of the channel.

4.2.3 Temperature Contour

For the temperature contour we follow the same procedure as that of previous case except temperature is selected as the variable which appears as below:

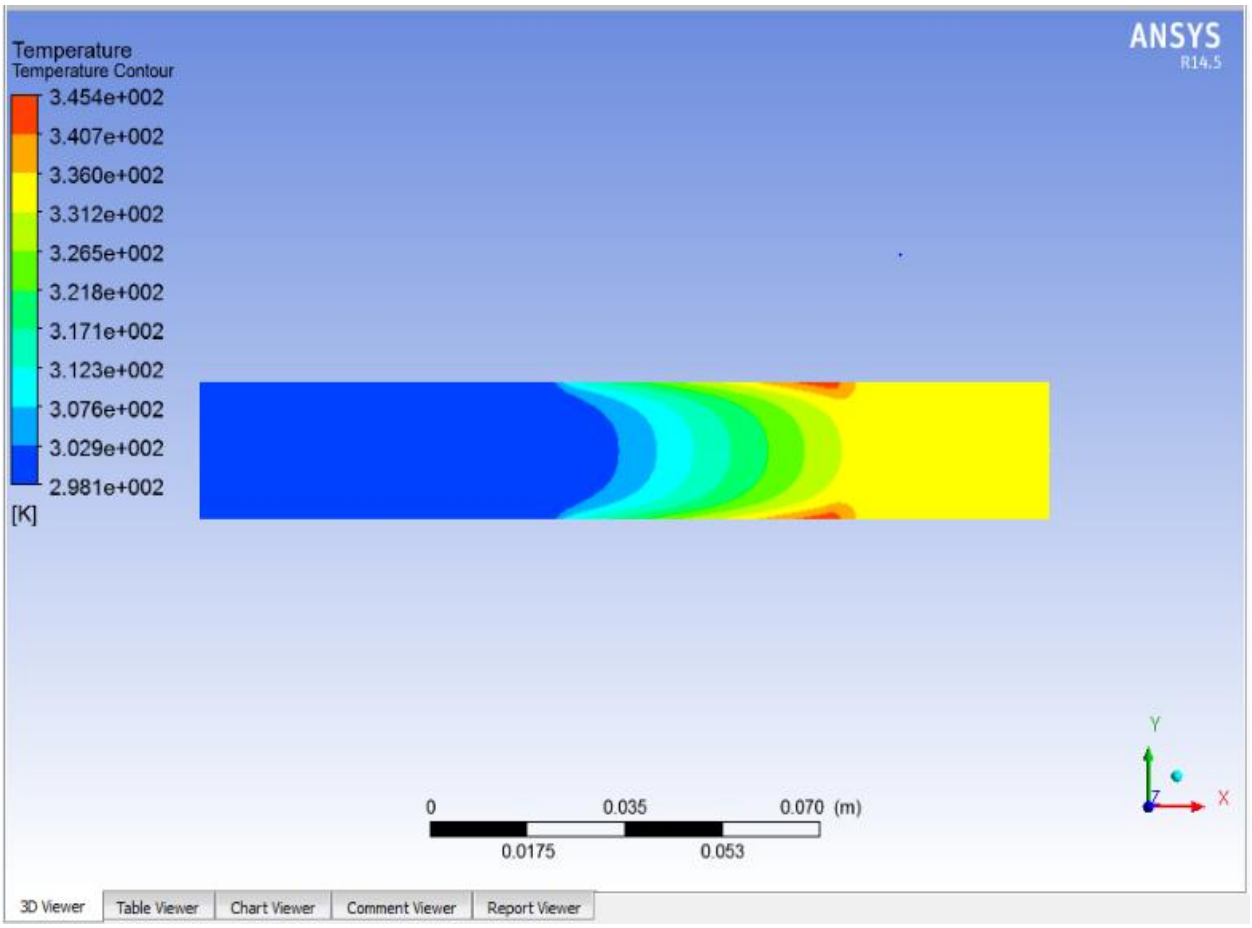

Fig. 4.3 temperature contour

The minimum value of temperature is 298.15 K which is at the inlet of the channel. While the maximum value of temperature is 345.404 K which is near the wall and at end of the heated region of microchannel.

4.2.4 Pressure Contour

Pressure is set as variable while all process remains the same. Pressure contour appears as below:

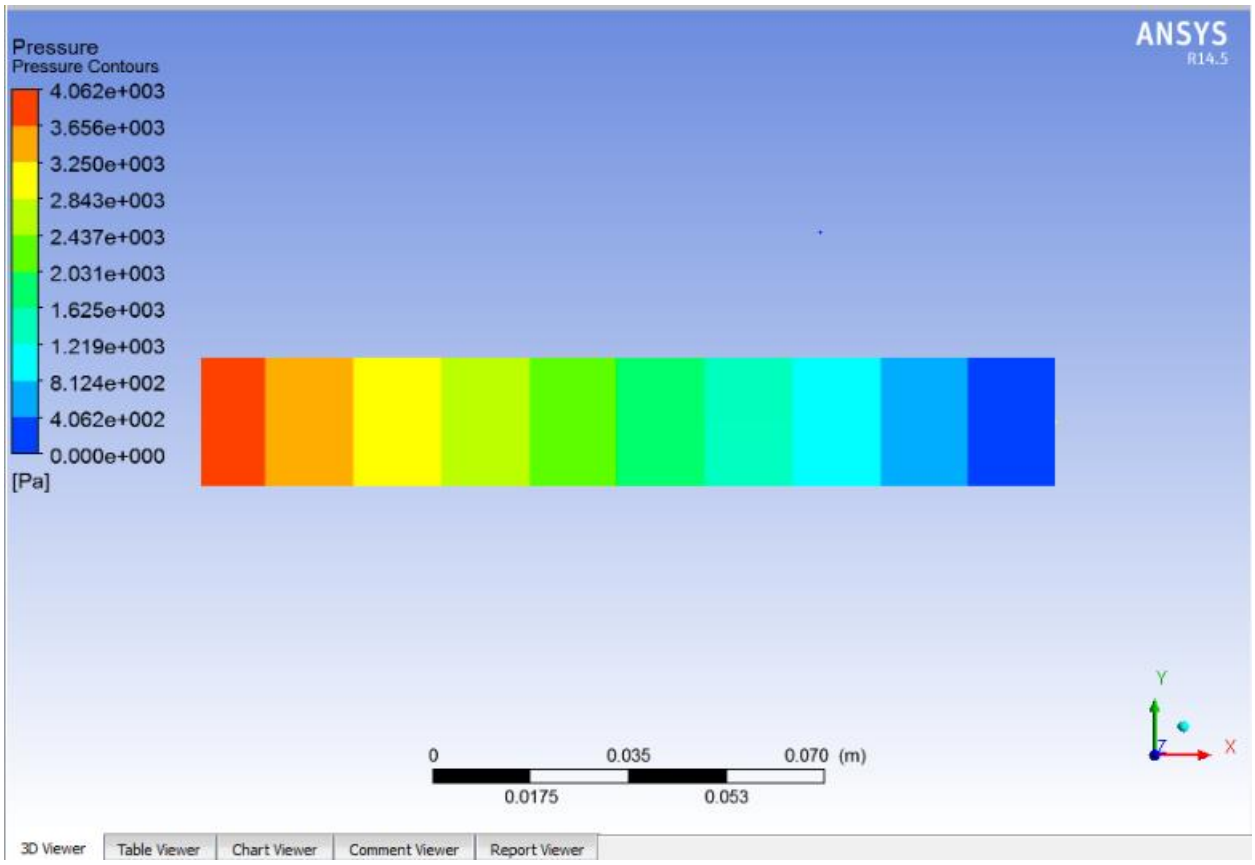

Fig. 4.4 pressure contour

The maximum value of gauze pressure is 4062.1 Pa which is at the inlet of the channel while the minimum value of gauze pressure is 0 Pa which is at the outlet of the channel as our operating condition is atmospheric pressure. As per the prediction, pressure decreases in the direction of flow.

4.2.5 Graph of Temperature along Centerline

For plotting graph along the centerline first of all we need to specify the line along which we want to plot the variation of temperature. So under location, line is selected and two point method is selected for specifying the centerline. 1st point is specified as (0, 0, 0) and 2nd as (0.1524, 0, 0). For more accurate results we specify no of samples to be 100. Under data series tab, centerline is selected as location, x is selected as variable for X axis tab and temperature is selected as variable for Y axis tab. On providing these many inputs we get the variation of temperature along centerline shown as below:

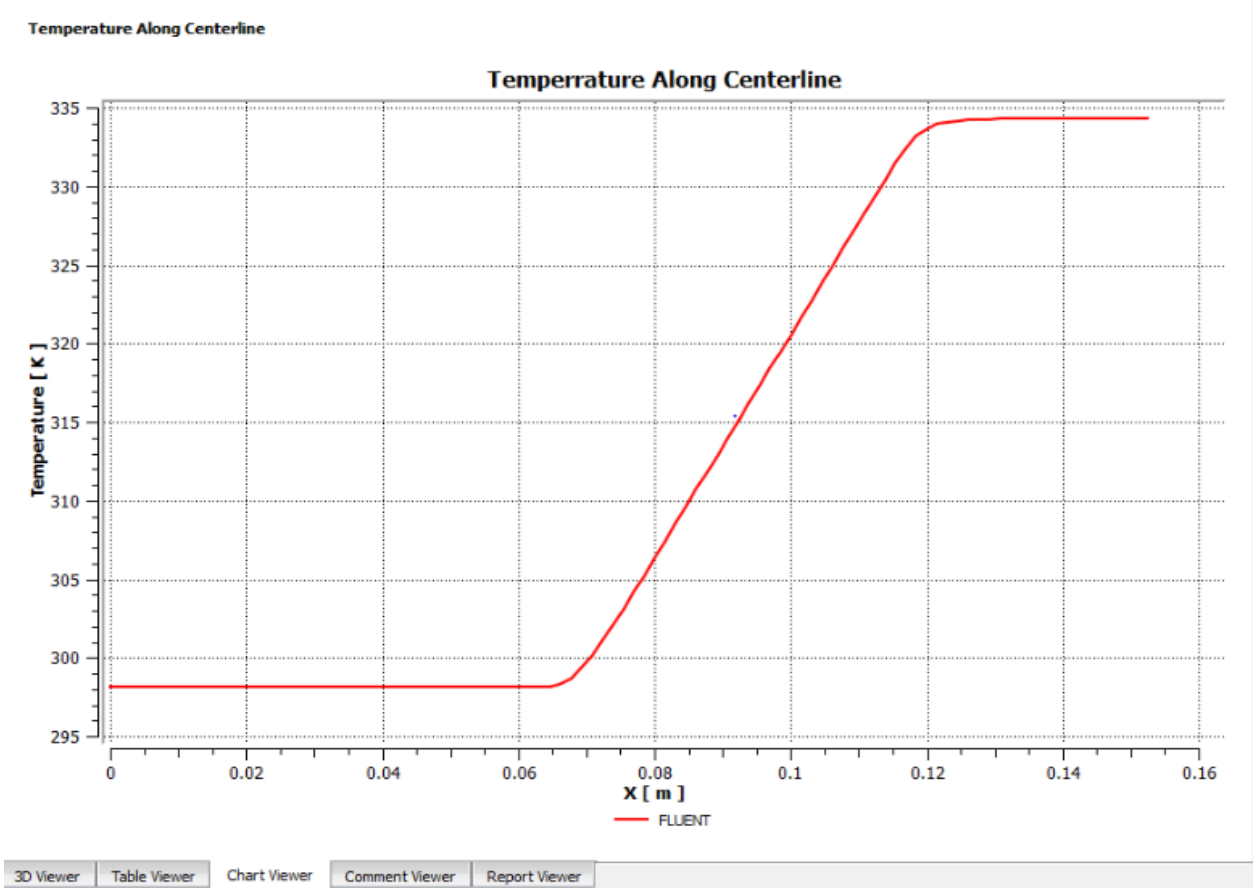

Fig. 4.5 Temperature variation along centerline

4.2.6 Graph of Temperature along Outlet

For plotting variation of temperature along outlet, first of all we need to create a line along the outlet of the channel. From location icon, line is selected and two point is selected for the method which is specified as point 1 (0.1524, 0, 0) and point 2 as (0.1524, 0.00038, 0). No of samples is selected as 100. Thus a line with the name of outlet is created. Now under data series tab, outlet is specified as location, temperature is selected as variable for X axis tab and Y is selected as variable under Y axis tab. When these many data variation of temperature is plotted which appears as below:

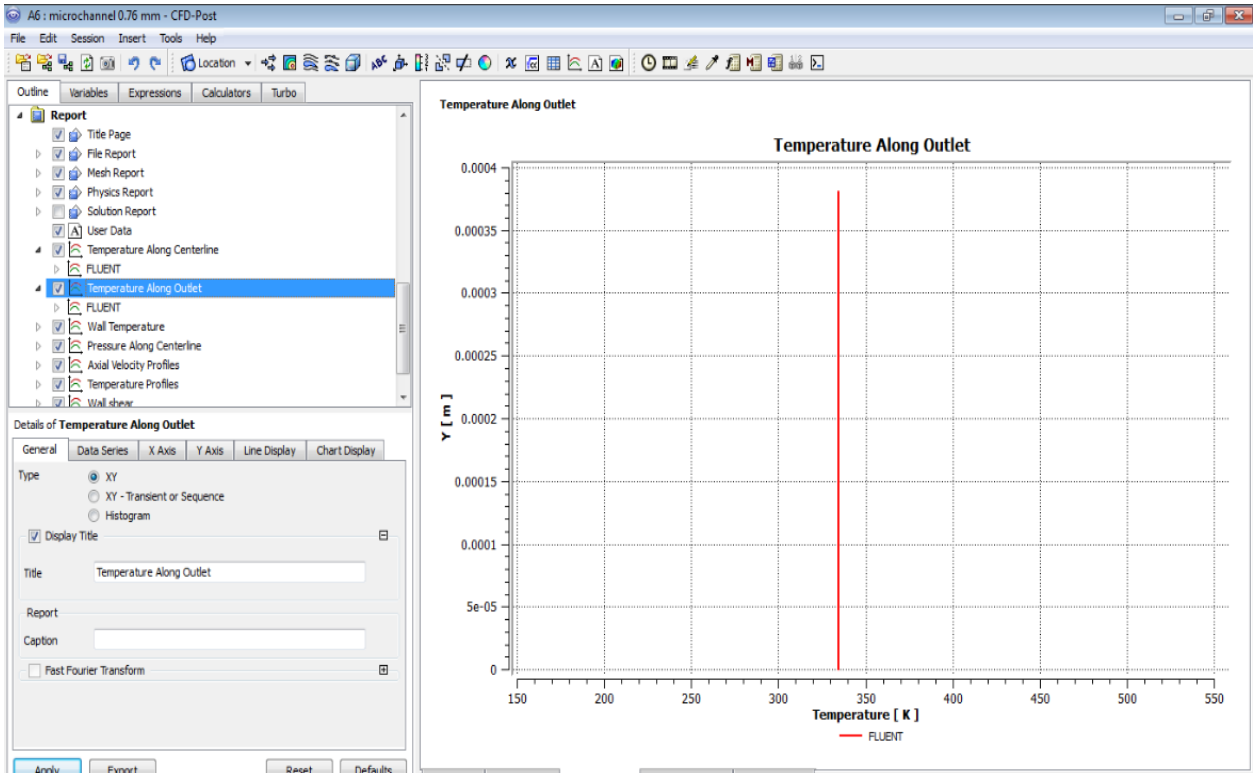

Fig. 4.6 graph of temperature at outlet

As it is obvious from the graph temperature at the outlet of the channel is constant.

4.2.7 Wall Temperature Variation

Again for this purpose we need to create another separate line. Under location tab we select line and name it as wall and two point method is selected as method for drawing line. The two point for line named wall is specified as point1 (0, 0.00038, 0) and point2 as (0.1524, 0.00038, 0). No of samples is selected as 100. On applying these data line named outlet is created. Now for plotting wall temperature variation under data series tab, wall is selected as location, temperature is selected as variable under X axis tab and temperature is selected as variable under Y axis tab. Graph of wall temperature appears as below:

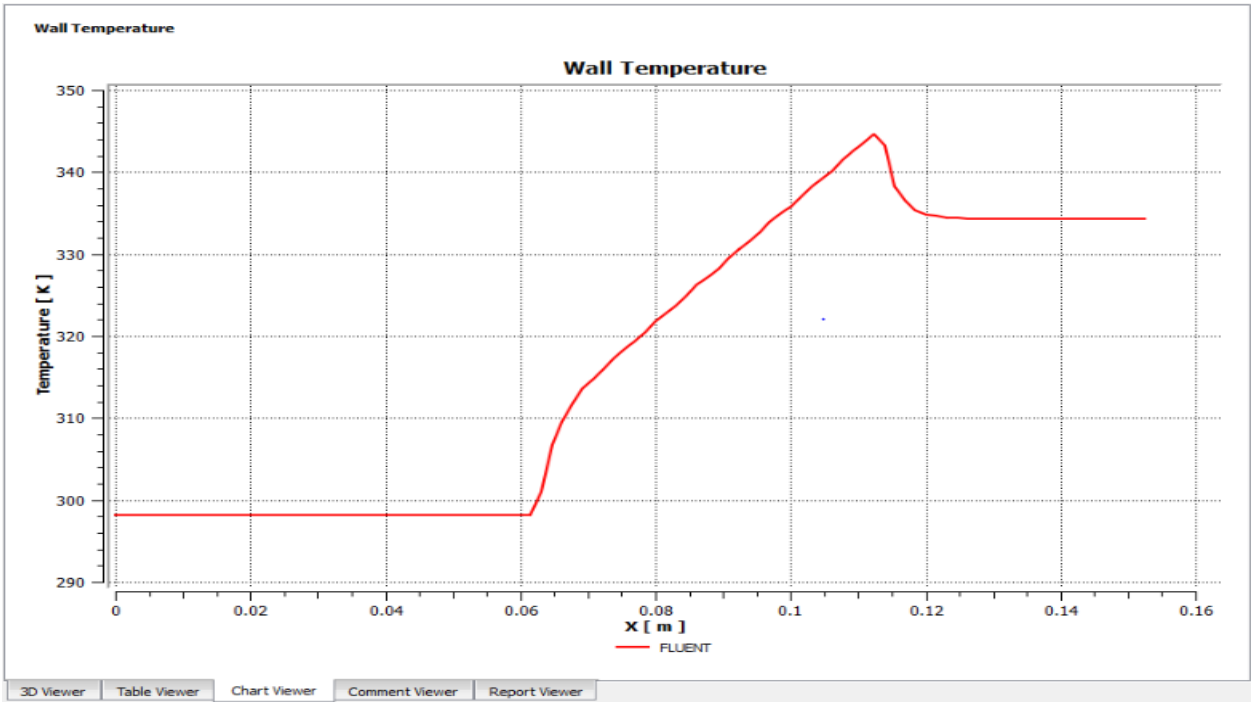

Fig. 4.7 wall temperature variation

4.2.8 Pressure Plot along Centerline

As centerline is already created we just need to specify centerline as location and X as variable for x axis tab and pressure as variable for Y axis tab. With all these data the variation of pressure along centerline is plotted which appears as below:

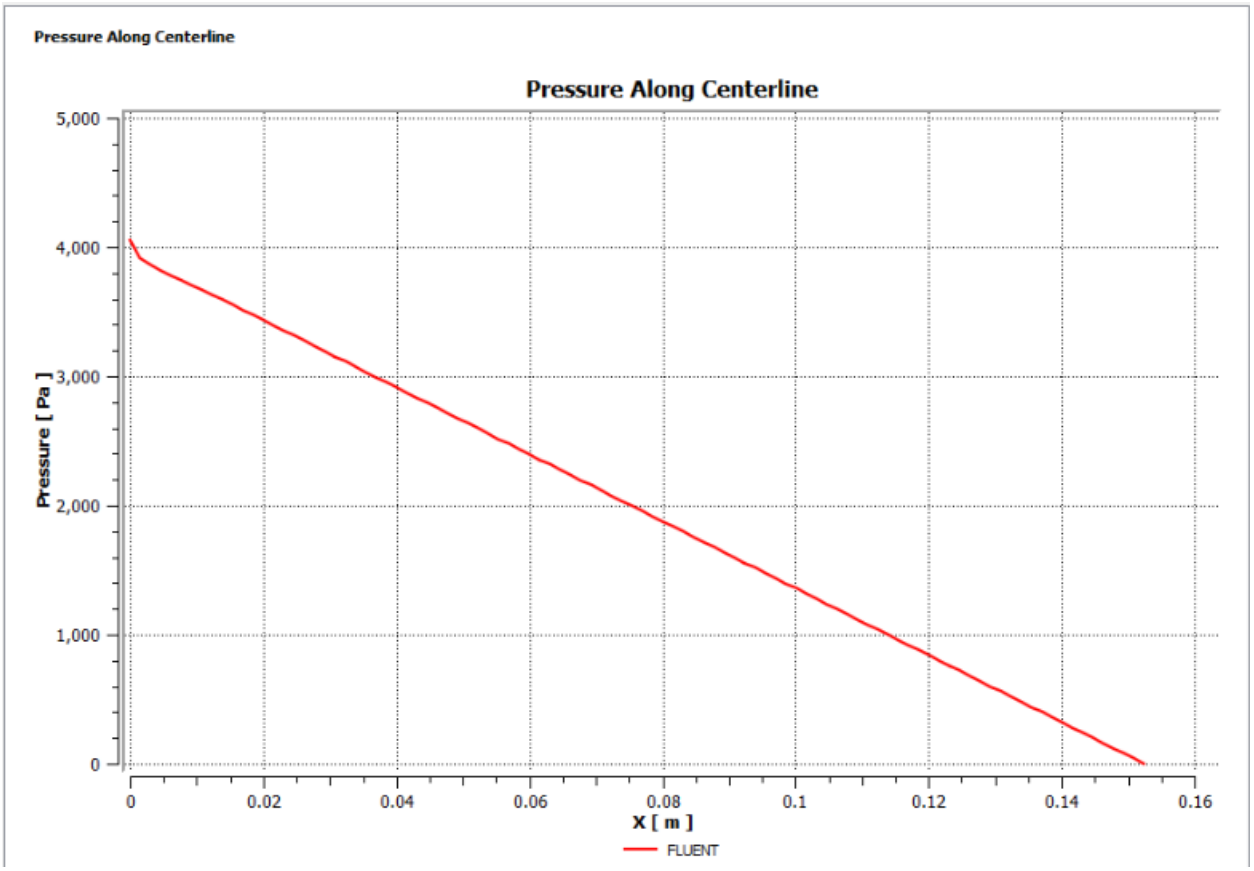

Fig. 4.8 pressure along centerline

4.2.9 Axial Velocity Profile

In this section we plot axial velocity profile at three different locations. For this purpose first of all three different line is created with name x0635, x1143 and x1524 at x= 0,0635m, x= 0.1143m and x=0.1524m respectively in the same

manner as described in previous sections. Under data series x1524, x1143 and x1542 is specified as location. Velocity u is selected as variable under X axis tab and Y is selected as variable under Y axis tab. With these data axial velocity profile for three different location is obtained in the same graph by inserting chart which appears as below:

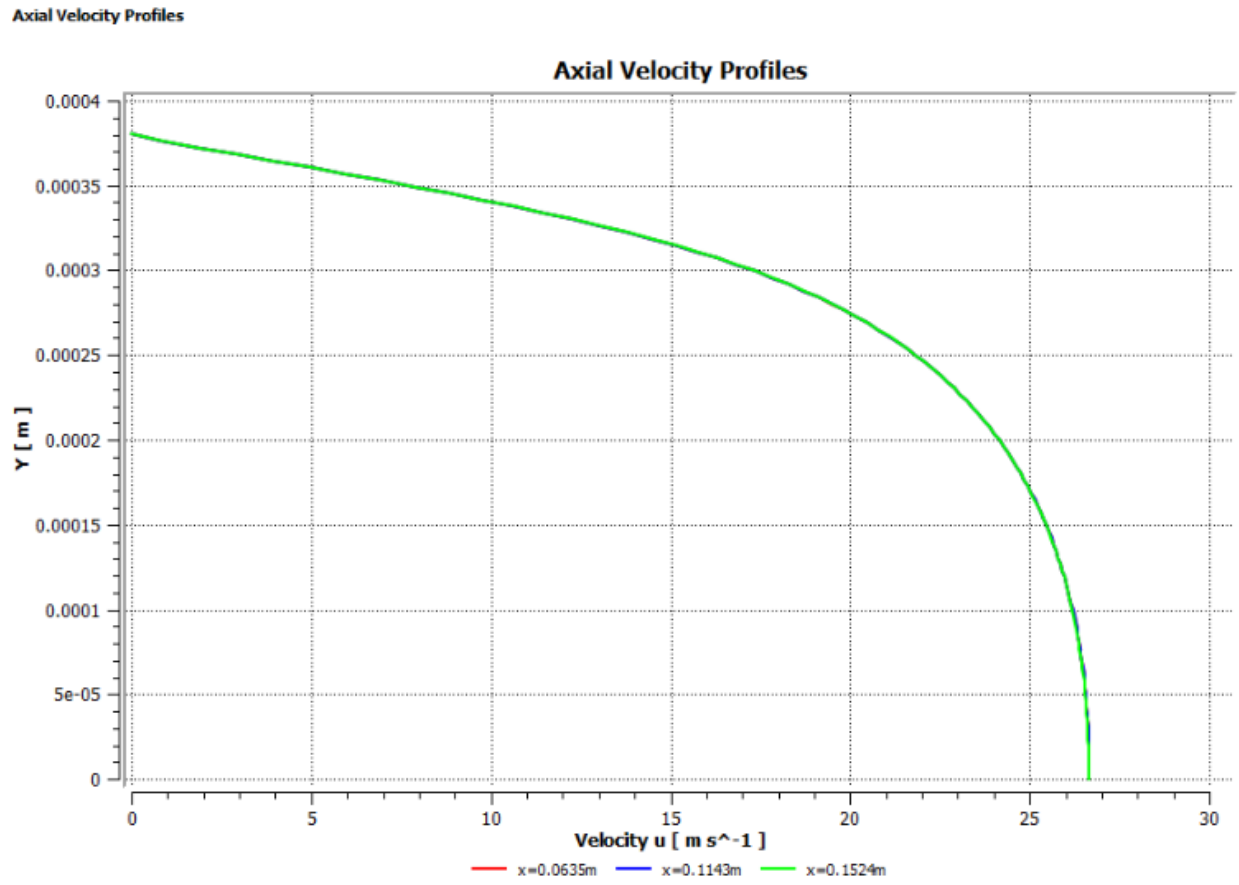

Fig. 4.9 axial velocity profile at x=0.0635m, x=0.1143m and x=0.1524m

As it can be seen all three graphs superimpose each other showing that at all three locations we have same axial velocity profile.

4.2.10 Temperature Profiles

In this section we are going to plot the variation in temperature at the three different locations for which lines have already been created in the previous section at x= 0.0635m, x=0.1143m and x= 0.1542m. All process are same as that of the previous case except for the fact that in this case temperature is selected as variable under X axis tab while Y is selected as variable under Y axis tab. The temperature profiles appear as below:

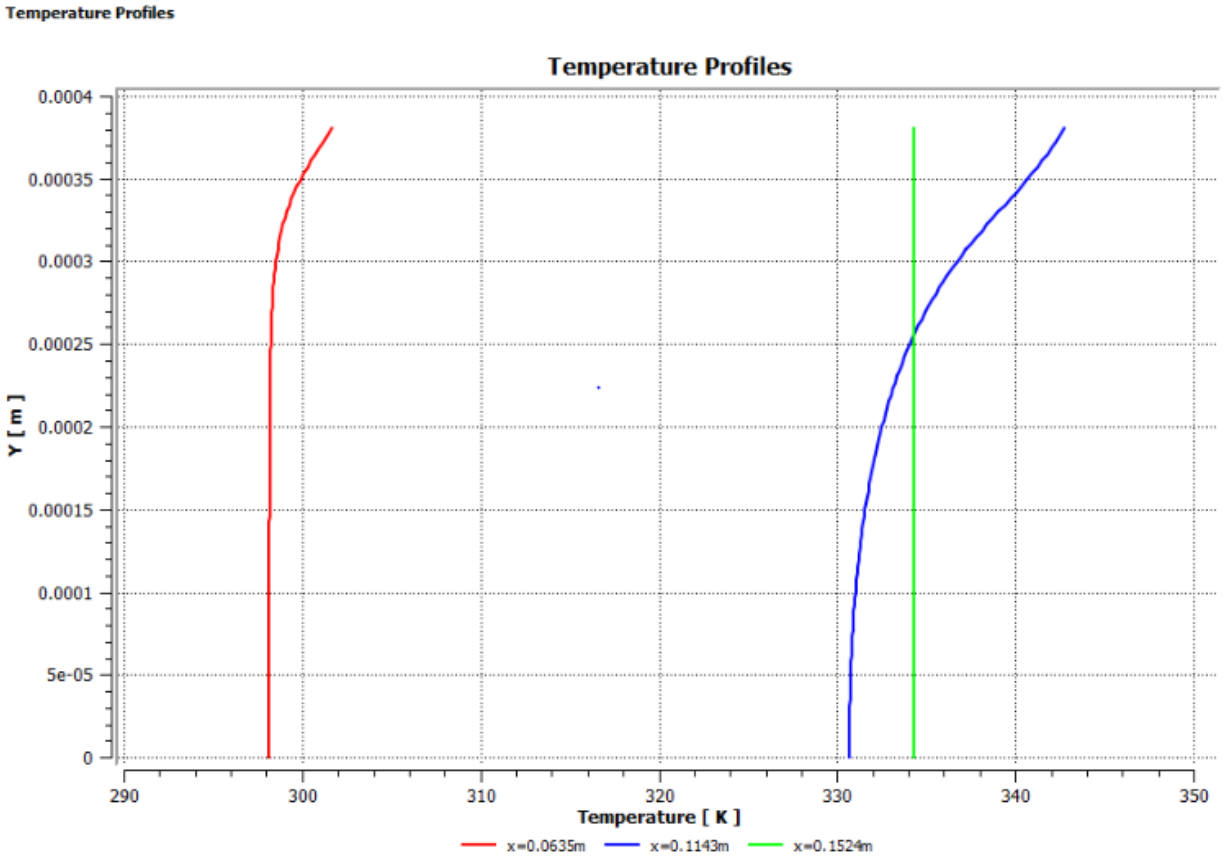

Fig. 4.10 temperature profiles at x= 0.0635m, x=0.1143m and x= 0.1542m

It is obvious from the graph that as we move closer to the wall of channel temperature increases and temperature is constant at the exit of channel which

complies with the graph drawn earlier under the heading “graph of temperature along outlet”. At the beginning of the cross section where heating starts increase in temperature is less while at the cross section where heating region ends increase in temperature is more which is obvious.

4.2.11 Wall Shear

The line named wall has already been created. So under data series tab wall is specified as the location. X is selected as variable for X axis tab while Wall Shear is selected as variable under Y axis tab. When above said conditions are applied the variation of wall shear is obtained as below:

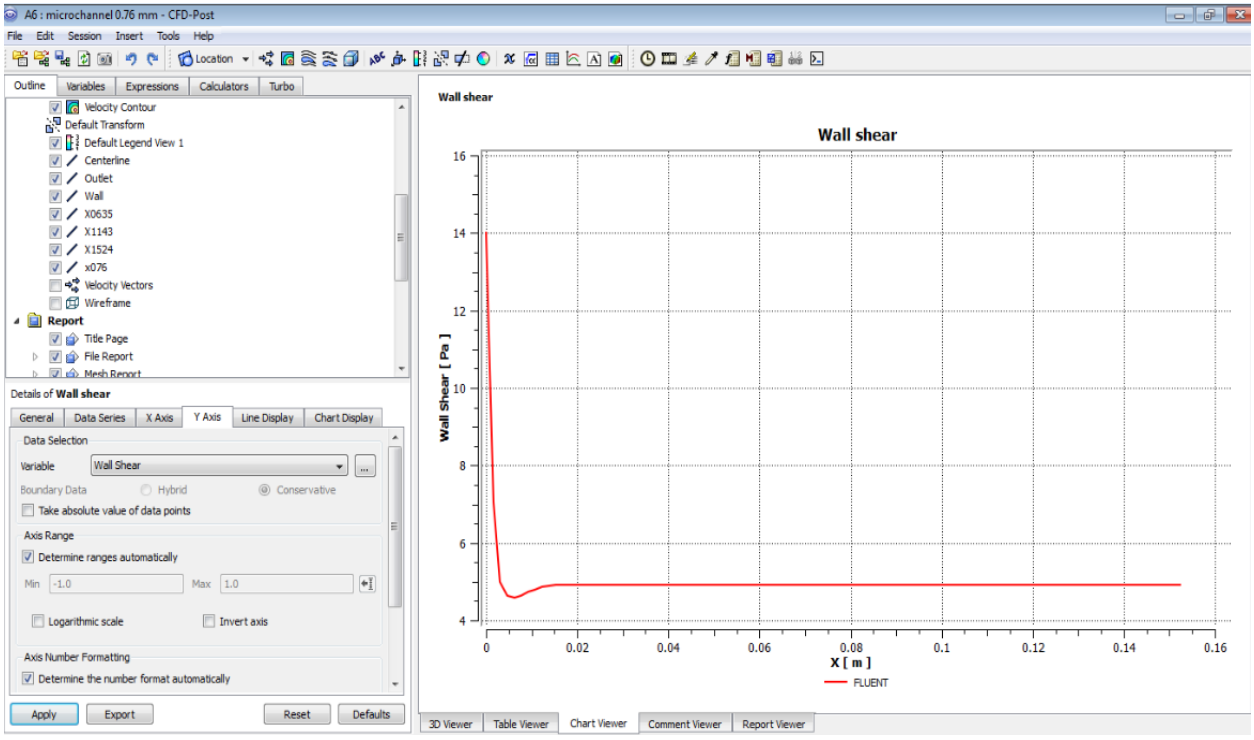

Fig. 4.11 wall shear variation

4.3 Model Validation

4.3.1 Grid Independence Test

The model is tested for grid-independence to give proper resolution to the region where large gradients of fluid flow and heat transfer characteristic is predicted. A grid independence test was carried out by increasing the number of nodes and cells and decreasing the element size for the microchannel heat sink which is given in table below:

model	Nodes	Element size	Cells	Faces	Minimum orthogonal quality	Maximum aspect ratio
Model 1	5549	8.82e^-4	5340	10888	1.0000e^00	2.75982e^2
Model 2	71053	8.82e^-5	69280	140332	9.74315e^-1	3.69106e^1

The fine grid mesh for the *x* and *y*-directions is adopted to properly resolve the velocity and viscous shear layers and to more accurately define the heat transfer at the surface of the channel, thereby improving the temperature resolution. CPU time as well as the memory storage required increases dramatically as the number of grid nodes is increased. However results and graphs obtained upon refining the mesh is approximately similar and very close to the previous results which confirm the grid independence of the present simulation.

4.3.2 Model Validation with Previous Experimental Studies

4.3.2.1 Nusselt Number Calculation

Nusselt number is a non dimensional number which provides us information regarding convective heat transfer. Expression for convective heat transfer at the channel wall is give as below:

$$q''_w = h(T_w - T_m) \quad \text{..... (10)}$$

From the above expression convective heat transfer coefficient is found as below:

$$h = \frac{q''_w}{(T_w - T_m)} \quad \text{..... (11)}$$

When we put the value of convective heat transfer in the expression of Nusselt number expression changes as below:

$$Nu = \frac{hL}{k} = \frac{q''_w(2R)}{k(T_w - T_m)} \quad \text{..... (12)}$$

Where

h is the convective heat transfer coefficient.

k is thermal conductivity of water.

L is the characteristic length. For the circular channel it is the diameter of the channel.

q"_w is the heat flux to which heated wall of microchannel has been subjected.

Tw is the temperature of channel wall at a given location.

Tm is mean temperature in the channel at the same location where Tw has been defined.

4.3.2.1.1 Calculation of Tw

For calculating Tw we need to tell FLUENT the location where it has to be found. For this purpose, first of all we define a line named x076 which has to be drawn at x= 0.076m. Line is again drawn by two point method and the two points being as point1 (0.076, 0, 0) and point2 as (0.076, 0.00038, 0).

After drawing the line x076 we find the maximum value of temperature along this line. For this we open expression tab and it is named as Tw. Under its definition we use post processor function **maxVal( )@** . Within parenthesis variable is defined while location follows after @ symbol. In the present case temperature is defined as the variable and line x076 is specified as location. After applying, Tw is calculated which in the present case comes out to be 318.679 K.

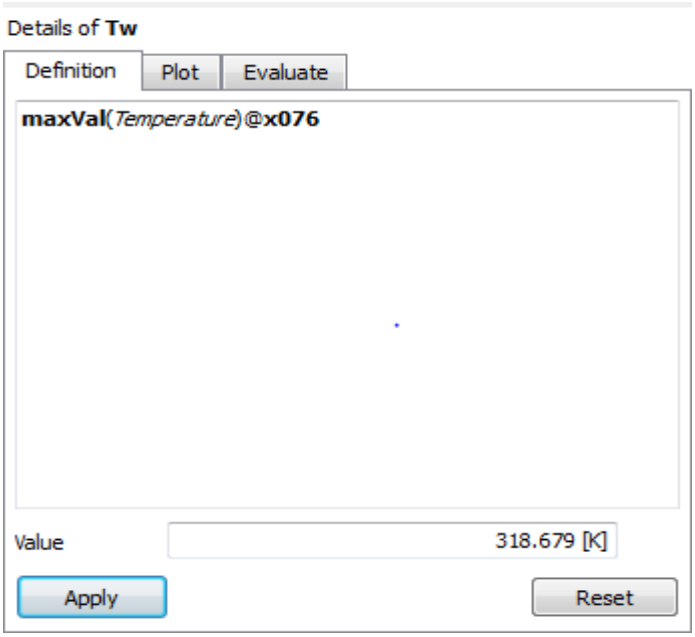

Fig.4.12 calculation of Tw

4.3.2.1.2 Calculation of Tm

To calculate mixed mean temperature at the same location we need not define the line or its location as it has already been defined. The mean temperature is calculated by using the concept of temperature which is area weighted average. For this concept of line integral is used in the FLUENT. The used concept is below:

$$\mathrm{Tm} = \frac{\int_0^R uT(2\pi r)\,dr}{\int_0^R u(2\pi r)\,dr} = \frac{\int_0^R urT\,dr}{\int_0^R ur\,dr} \quad \text{..... (13)}$$

For calculating Tm we click expression tab and define a new expression named Tm. In its definition the following expression is entered:

*lengthInt(Velocity u*Y*Temperature)@x076/ lengthInt(Velocity u*Y)x076*

On entering this expression and applying the Tm is calculated which is 307.055 K in the present case.

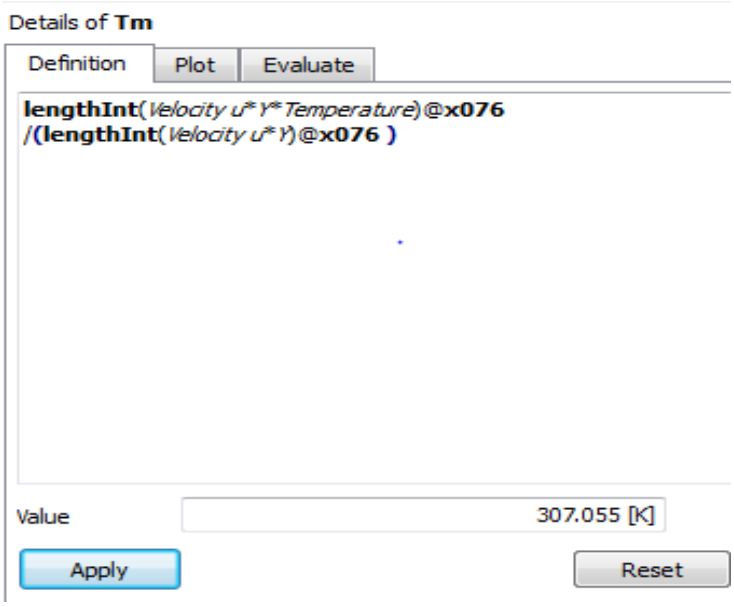

Fig. 4.13 calculation of Tm

Now we have all required data to calculate the Nusselt number. A new expressionnamed Nu is defined and in its definition values are put as per equation (10) defined above. We get the calculated value of Nusselt number as 251.147. This calculated value of Nu will be used to validate the present CFD modeling. The outline tree in CFD post processor showing the expression and calculated value of Nusselt number appears as below:

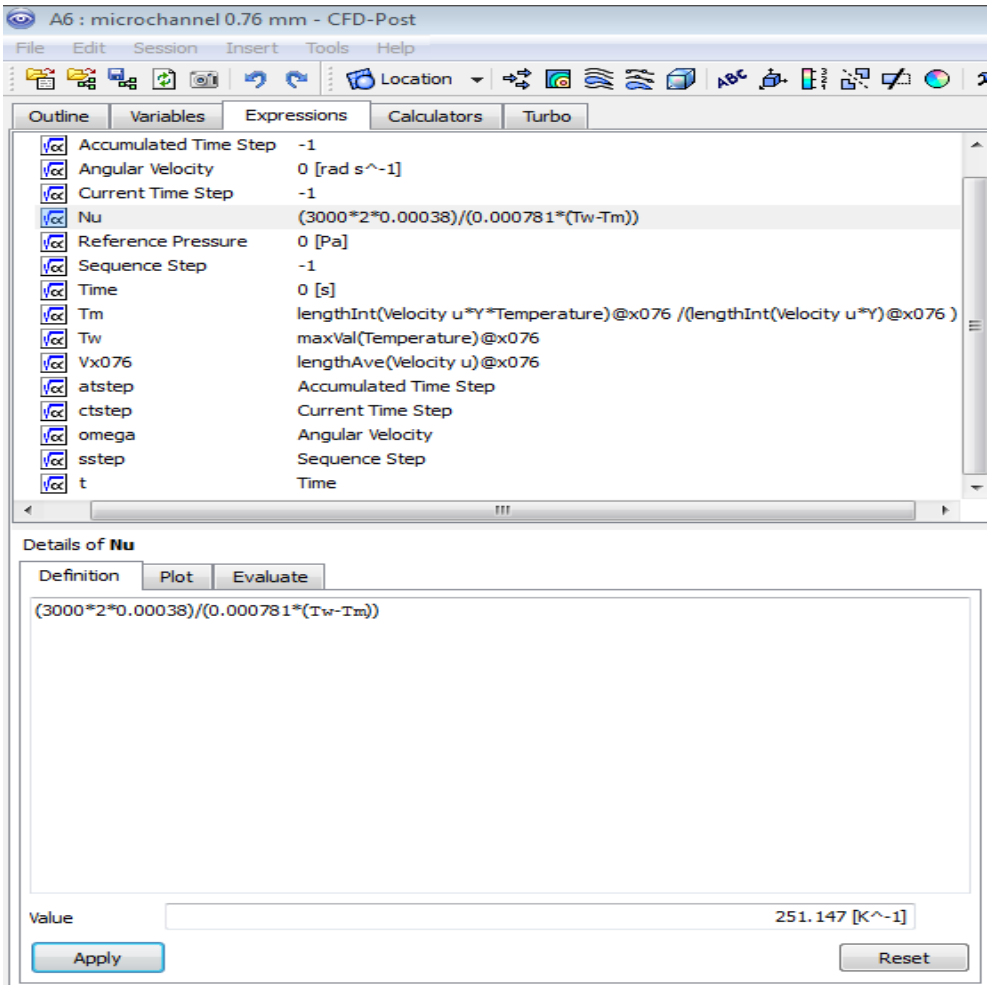

Fig. 4.14 Calculation of Nu

4.3.2.2 Validation of CFD Modeling

The present CFD model is validated by comparing the value of Nusselt number calculated by post processor of FLUENT to the value of Nusselt number that is

obtained from the correlations for the microchannel by T. M. ADAMS. In the experimental investigation conducted by T. M. ADAMS found that the value of Nu that is determined experimentally comes out to be much higher than the value that is calculated using conventional correlations. Gnielinski modified correlation given by Petukhov which is given as below:

$$Nu = \frac{(f/8)(Re-1000)Pr}{1+12.7(f/8)^{1/2}(Pr^{2/3}-1)} \quad \ldots\ldots (14)$$

Where

Nu is Nusselt number

Re is Reynolds number

Pr is Prandtl number

F is friction factor whose expression was given by Gnielinski as below:

$$f = (1.82\log(Re)-1.64)^{-2}. \quad \ldots\ldots (15)$$

In the present work, Nu was calculated by FLUENT in the microchannel at a location x=0.076m. We calculate Re and Pr in the microchannel for the same location. For calculating average Re, average velocity is calculated at x=0.076m.

Fig. 4.15 calculation of average velocity at x= 0.076m

Temperature at x=0.076 is found to be 307.055 K and correspondingly value of kinematic viscosity of water is 7.867*10^-7. With all these values Re comes out to be 20588.11.

From equation 15 the value of friction factor is found.

f = (1.82 log (20588.11)- 1.64)^-2

f = 0.02592

Putting the value of friction factor Nu is found from equation 14.

$$(Nu)G = \left[\left(\frac{0.02592}{8}\right) \times (20588.11 - 1000) \times (5.26)\right] \div \left[1 + (12.7) \times (0.02592 \div 8)^{0.5} \times \left(5.26^{\frac{2}{3}} - 1\right)\right]$$

$(Nu)_G = 135.50$

Nu value calculated by Gnielinski eqn. comes to be 135.50. T. A. ADAMS modified Gnielinski eqn. which is as below:

$$Nu = Nu_{Gn}(1 + F) \quad \text{..... (16)}$$

Where F is given by

$$F = CRe\left(1 - \left(\frac{D}{D_0}\right)^2\right) \quad \text{..... (17)}$$

Where

$C = 7.6 \times 10^{-5}$ and

$D_0 = 1.164$ mm

As per the work of T. A. ADAMS the error between the experimental result and the value as predicted by correlation given by eqn. 14 & 15 is $\pm$ 18.6 % .

$F = (7.6 \times 10^{-5}) \times (20588.11) \times [1 - (0.76 \div 1.164)^2]$

F = 0.89

The value of Nu as per T. A.ADAMS will be

$Nu = 135.50 \times (1 + 0.89)$

$Nu = 256.11$

The value of Nu calculated by FLUENT was 251.147. Therefore % error in the calculated value of Nu is

$[(256.11 - 251.147) / 251.147] \times 100$ = 1.78 %

The error in the value of Nu calculated experimentally i.e ; in this case by FLUENT and the value predicted by the correlation given by T. A. ADAMS comes out to be 1.78 % which is well in agreement with the work of T. A. ADAMS. Hence the present CFD modeling is validated.

5. SIMULATION of MICROCHANNEL of DIAMETER 1.09 mm

5.1 Introduction

As the above model has already been validated it can be used for simulation of other microchannels as well. In the present section analysis of fluid flow and heat transfer has been discussed for the microchannel of diameter of 1.09 mm. The velocity at the inlet is 18 m/s while the flux at the heated section is same as that of 3000 W/m^2. Length and other geometry parameter and boundary conditions remains the same. Experimental work on microchannel with diameter of 1.09 mm diameter has already been done by T. A. ADAMS. Geometry and meshing is done in the similar manner as above. Results of microchannel with 1.09 mm diameter are as below:

5.2 Velocity Vector

The velocity vector appears as below:

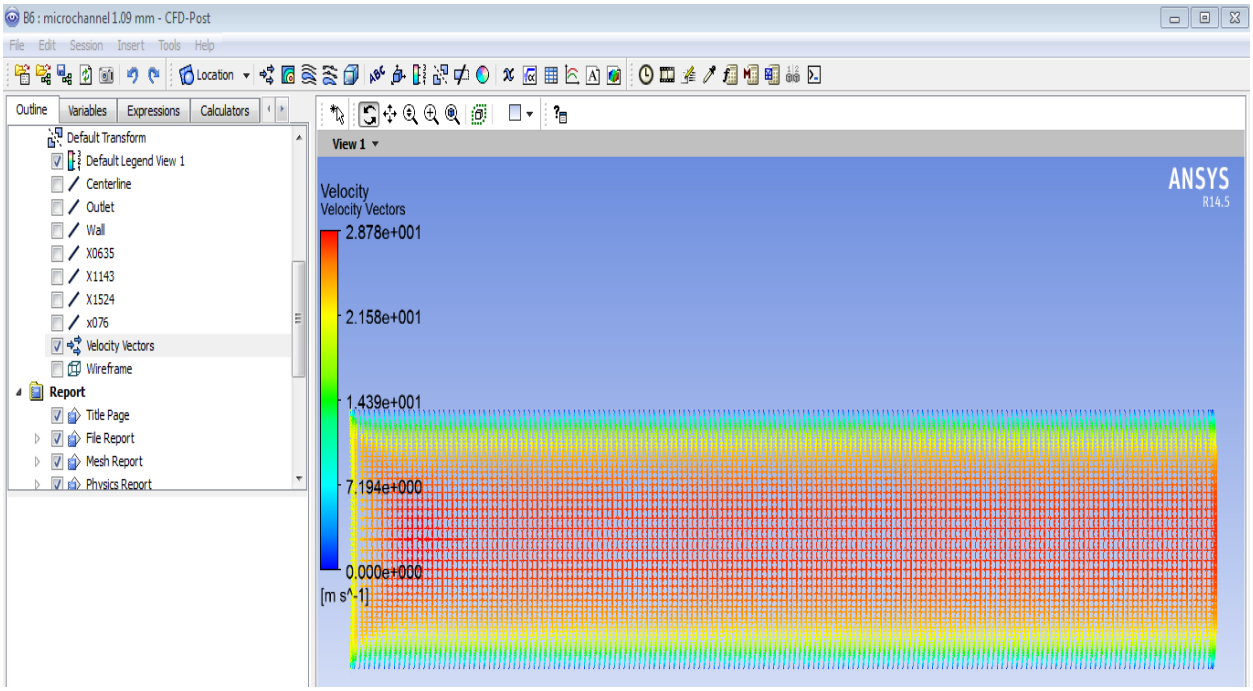

Fig. 5.1 variation of velocity vector

5.3 Velocity Contour

The velocity contour of microchannel appears as below:

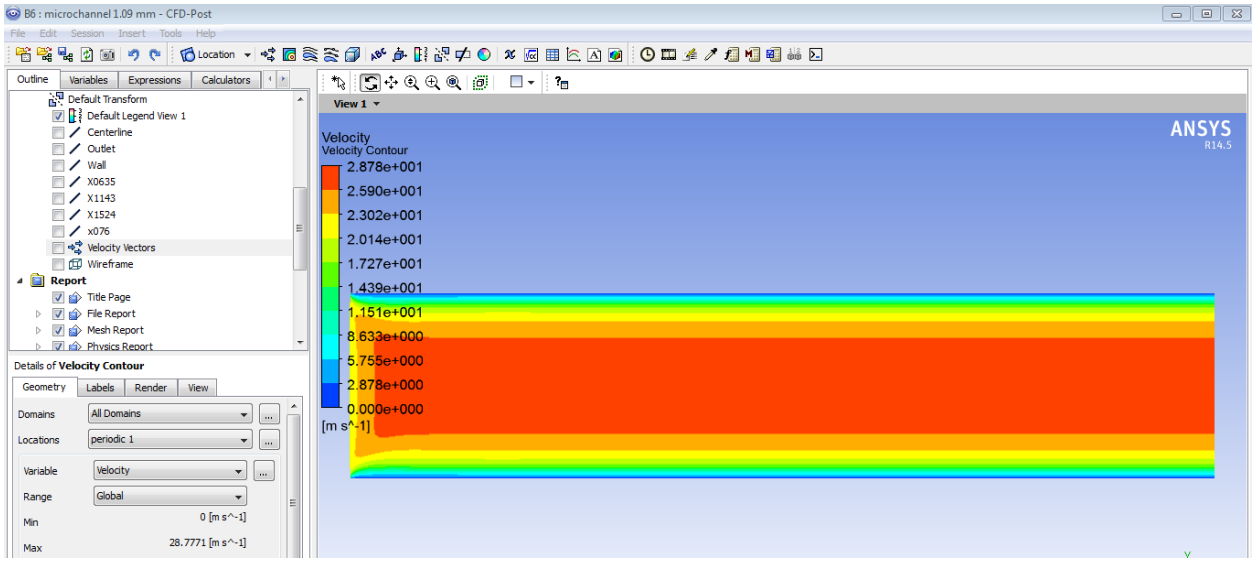

Fig. 5.2 velocity contour

Velocity is maximum near the axis and minimum at near the wall. Maximum value of velocity is 28.7771 m/s and minimum value is zero.

5.4 Temperature Contour

The temperature contour of the channel appears as below:

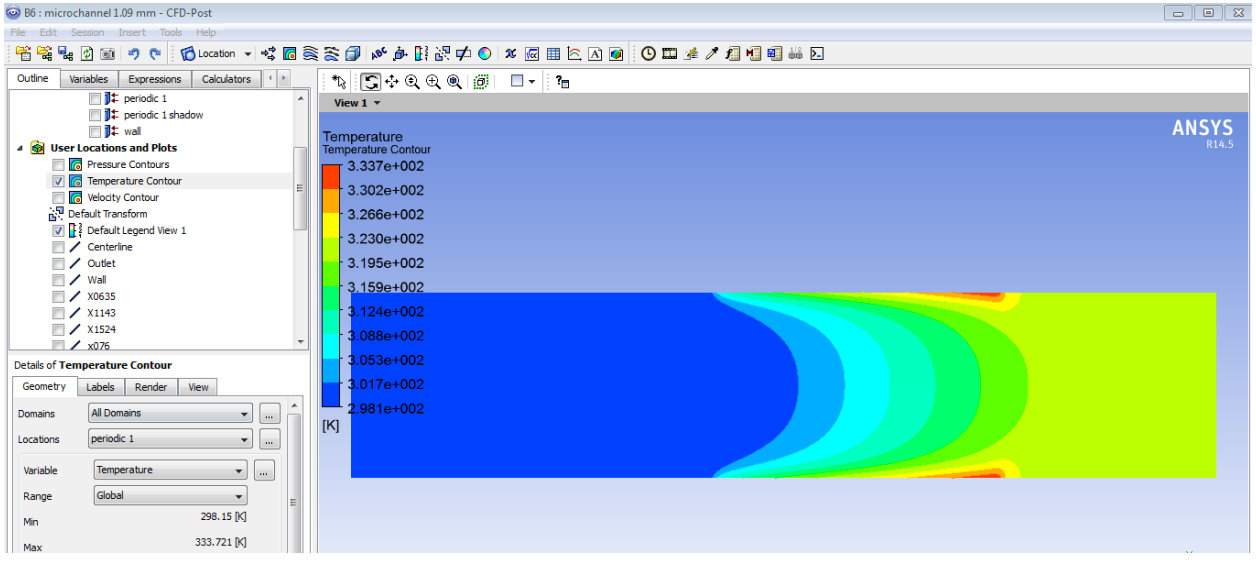

Fig. 5.3 temperature contour

Temperature increases in the heated section with the maximum and minimum value being 333.721 K and 298.15 K respectively. The maximum value is near the wall at the end of heated section while the minimum value is at the entry of the channel.

5.5 Pressure Contour

The pressure contour appears as below:

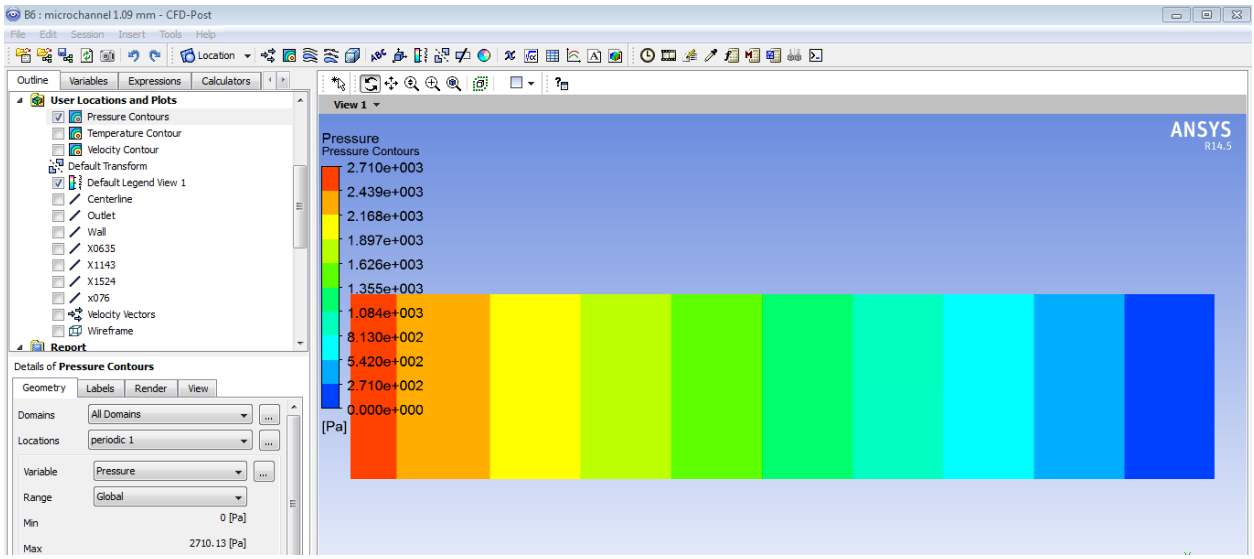

Fig. 5.4 pressure contour

Pressure decreases in the direction of flow. The maximum and minimum value being 2710.13 Pa and zero Pa in gauze pressure scale respectively.

5.6 Graph of Temperature Along Centerline

The variation of temperature along the centerline appears as below:

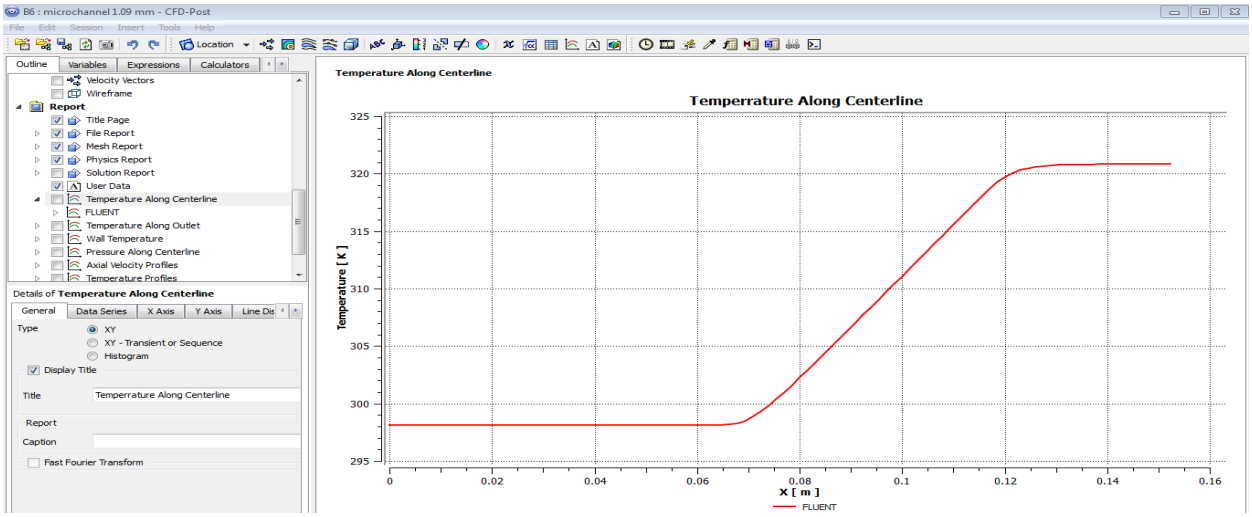

Fig. 5.5 temperature along centerline

Temperature along centerline increases in the heating region while remains constant in the remaining sections.

5.7 Wall Temperature Variation

The variation of wall temperature is plotted which appears as below:

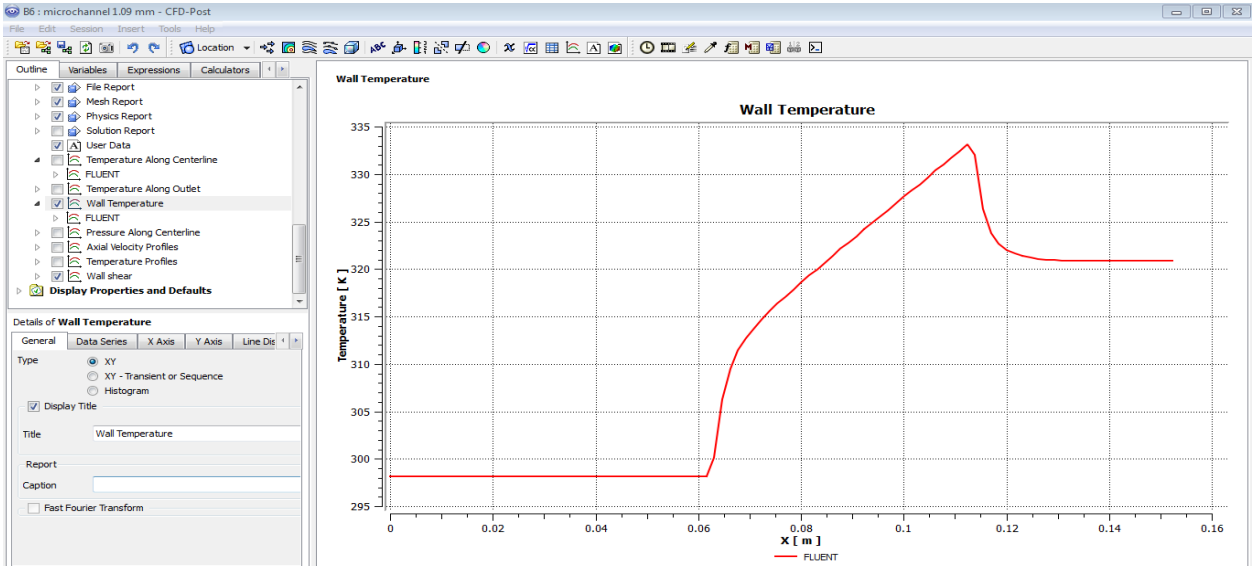

Fig. 5.6 wall temperature variation

5.8 Pressure Plot along Centerline

Variation in pressure along centerline is plotted which appears as below:

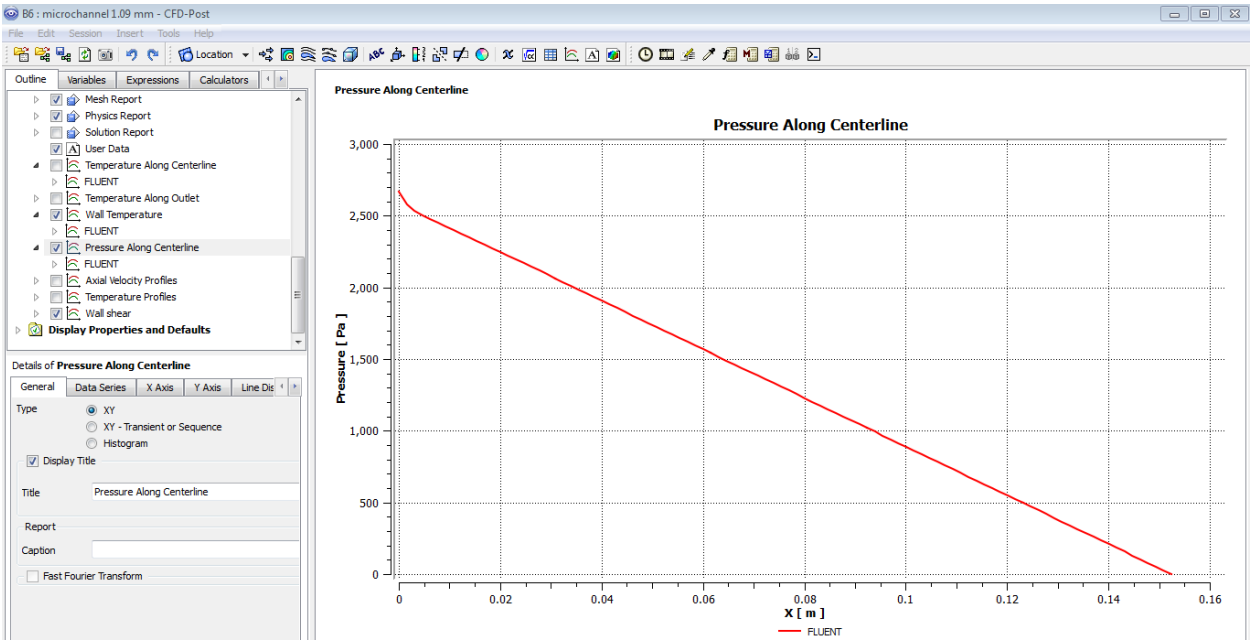

Pressure variation along centerline

Pressure falls continuously right from inlet of the channel till exit.

5.9 Axial Velocity Profile

Axial velocity variation of water inside the channel at three different locations namely at x = 0.0635m, x = 0.1143m and x = 0.1542m is plotted. Although all three graphs have been plotted with three different colours, in the fig. only one curve is seen because all three graphs being of the same nature, they overlap each other. The axial velocity profile appears as below:

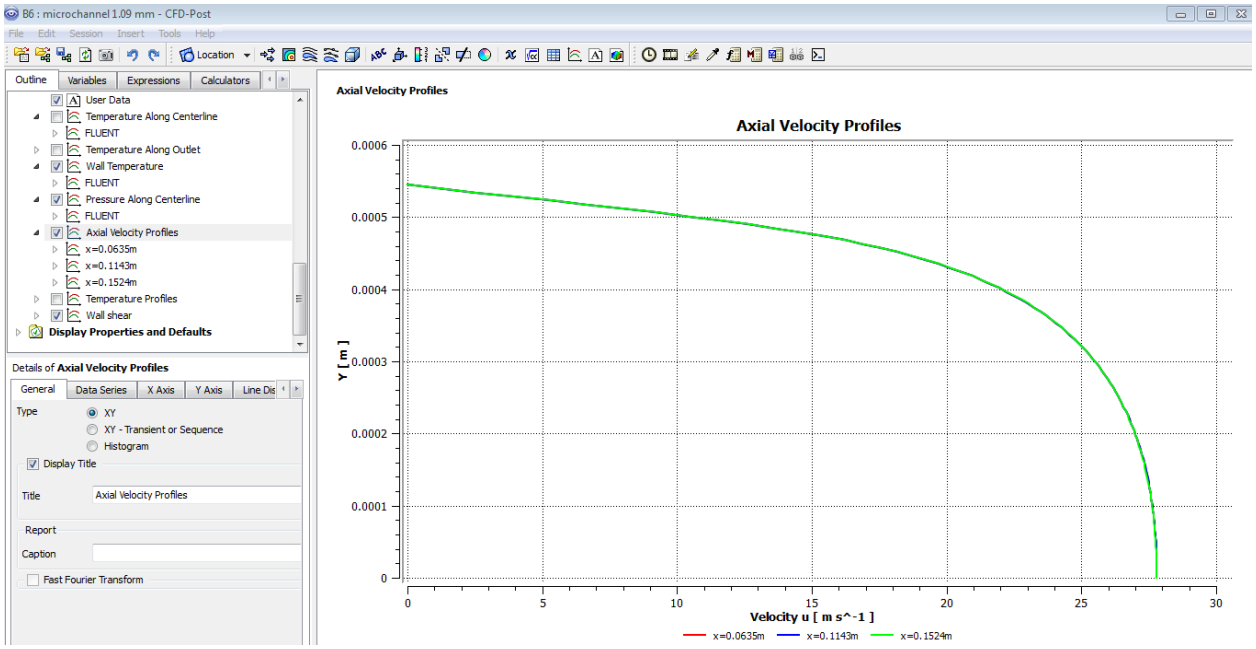

Fig. 5.9 Axial Velocity Profile

5.10 Temperature Profiles

Variation in temperature at three different locations in Y direction has been plotted which appears as below:

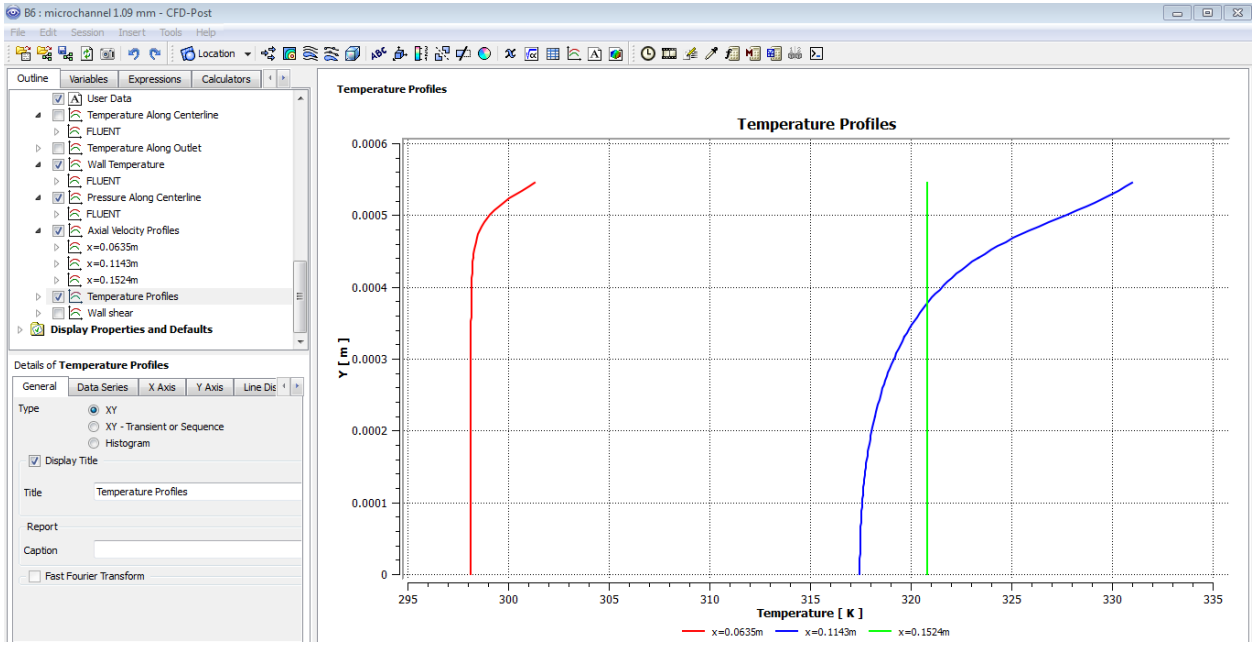

Fig. 5.9 temperature profile

5.11 Variation of Wall Shear

Variation in wall shear is plotted in the direction of flow which appears as below:

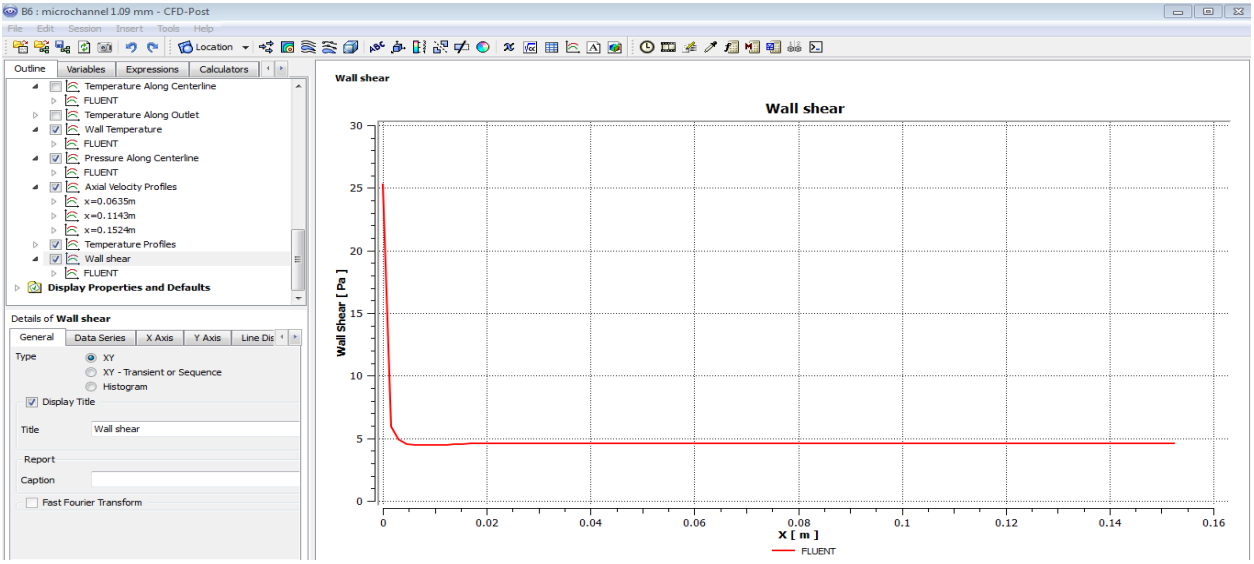

Fig. 5.10 wall shear

The wall shear value falls in flow development region, rises a little bit and thereafter it remains constant.

5.12 Nusselt Number Calculation:

Nusselt number at X = 0.076m is calculated with the help of fluent. The method of calculating the Nusselt number is the same as that of previous channel with diameter 0.76mm diameter. Tw in the present case comes out to be 316.566 K.

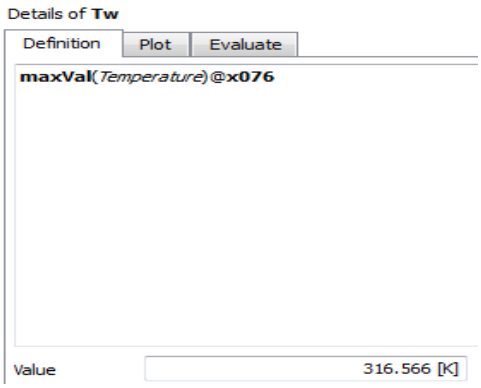

Fig. 5.11 calculation of Tw

The mean temperature comes out to be 303.742 K.

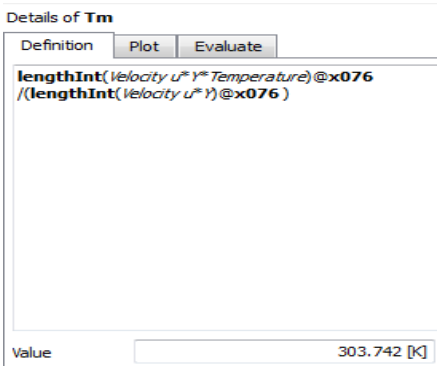

Fig. 5.12 calculation of Tm

With the help of Tw and Tm value of Nusselt number is calculated with the help of eqn. 12 which in the present case comes to be 299.289.

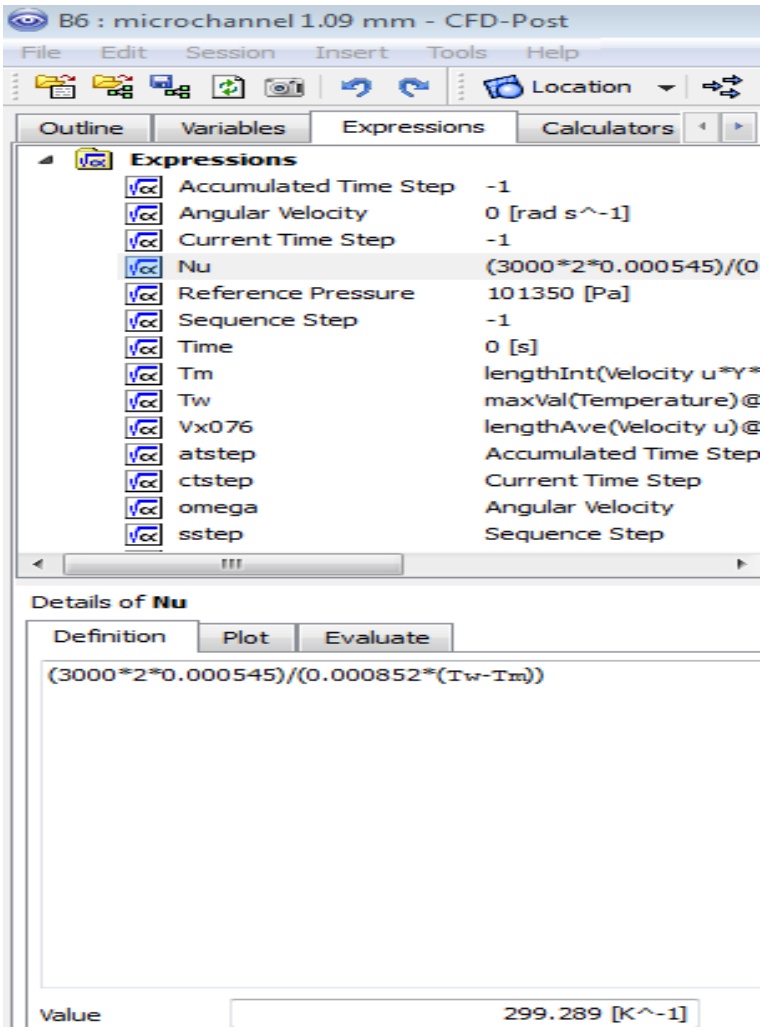

Fig. 5.13 Nusselt number

Again nusselt number is calculated using Gnielinski correlation using eqn. 14 & 15.

f = (1.82 log (29324.5)- 1.64)^-2

f = 0.02374

$(\quad Nu)G = \left[\left(\frac{0.02374}{8}\right) \times (29324 - 1000) \times (5.841)\right] \div \left[1 + (12.7) \times (0.02374 \div 8)^{0.5} \times \left(5.841^{\frac{2}{3}} - 1\right)\right]$

$(Nu)_G = 192.7$

Now Nu as per T. A. ADAMS' is calculated as per eqn. 16 & 17.

$F = (7.6 \times 10^{-5}) \times (29324.5) \times [1 - (1.09 \div 1.164)^2]$

F = 0.27

The value of Nu as per T. A. ADAMS will be

$Nu = 192.7 \times (1 + 0.27)$

$Nu = 245.57$

The value of Nu calculated by FLUENT was 299.289. Therefore % error in the calculated value of Nu is

$[(299.289 - 245.57) \div 289] \times 100 = 17.9\ \%$

The error in the above value is less than $\pm$ 18.6 % which is well in agreement with the work of T. A. ADAMS.

6. SIMULATION of MICROCHANNEL of DIAMETER 0.76 mm with AIR as a COOLANT.

6.1 Introduction

The modeling and boundary conditions everything is the same as in the case of microchannel o.76 mm diameter with water as coolant. With this analysis we can compare the results obtained while using two different coolant. Results of microchannel with air as a coolant are as below:

6.2 Velocity Vector

Plot of velocity vector using air as the coolant appears as below:

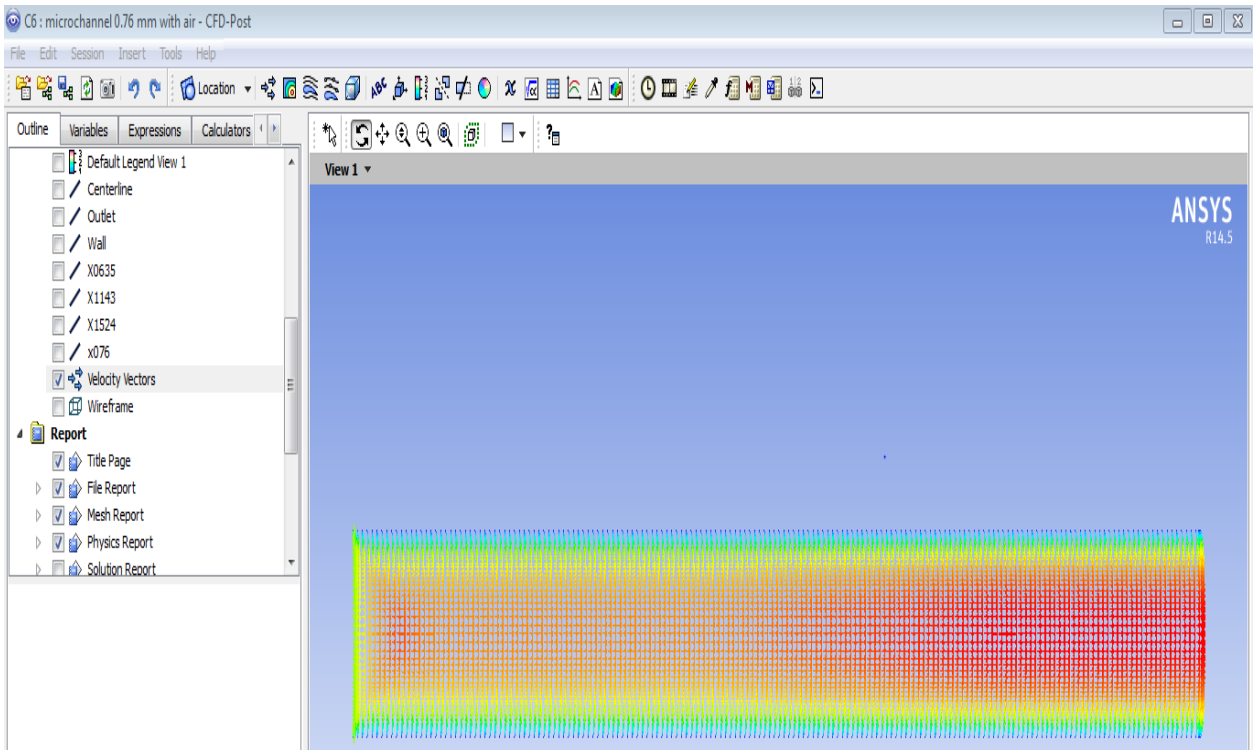

Fig. 6.1 velocity vector

6.3 Velocity Contour

Velocity contours appears as below:

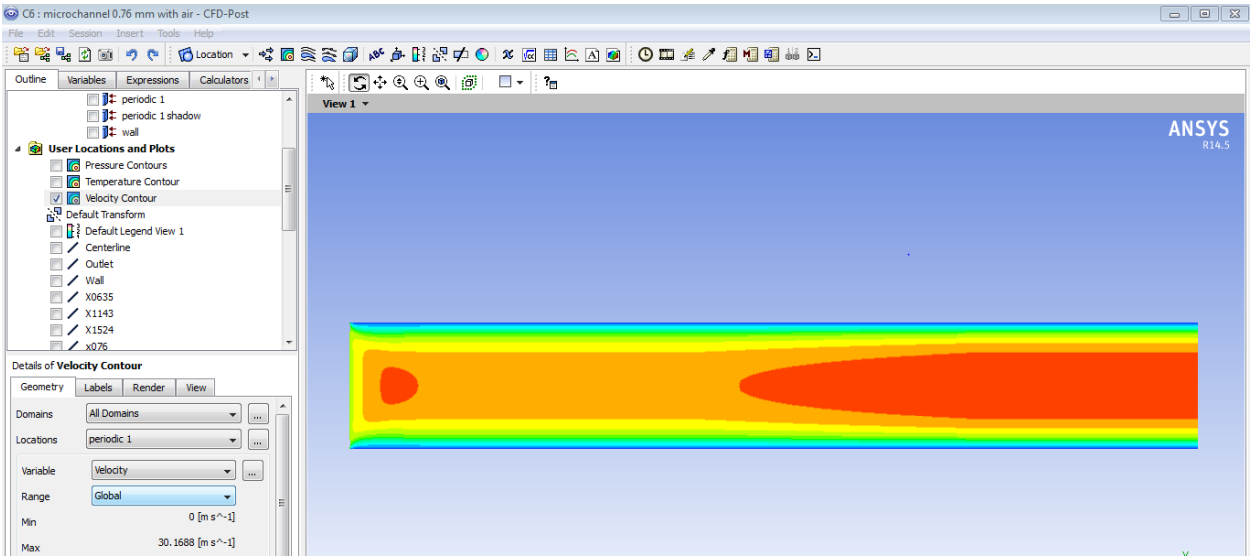

Fig. 6.2 velocity contour

Velocity of air is the maximum at exit and the minimum value is near to the wall as fluid is in no slip condition. The maximum and minimum values of velocity in the entire flow regime are 30.1688 m/s and zero respectively.

6.4 Temperature Contour

The temperature contour tells us the temperature variation in the entire region. In the present case using air as the coolant the maximum and minimum temperature in the entire flow regime is 346.399 K and 298.15 K respectively. The temperature contour in the present case appears as below:

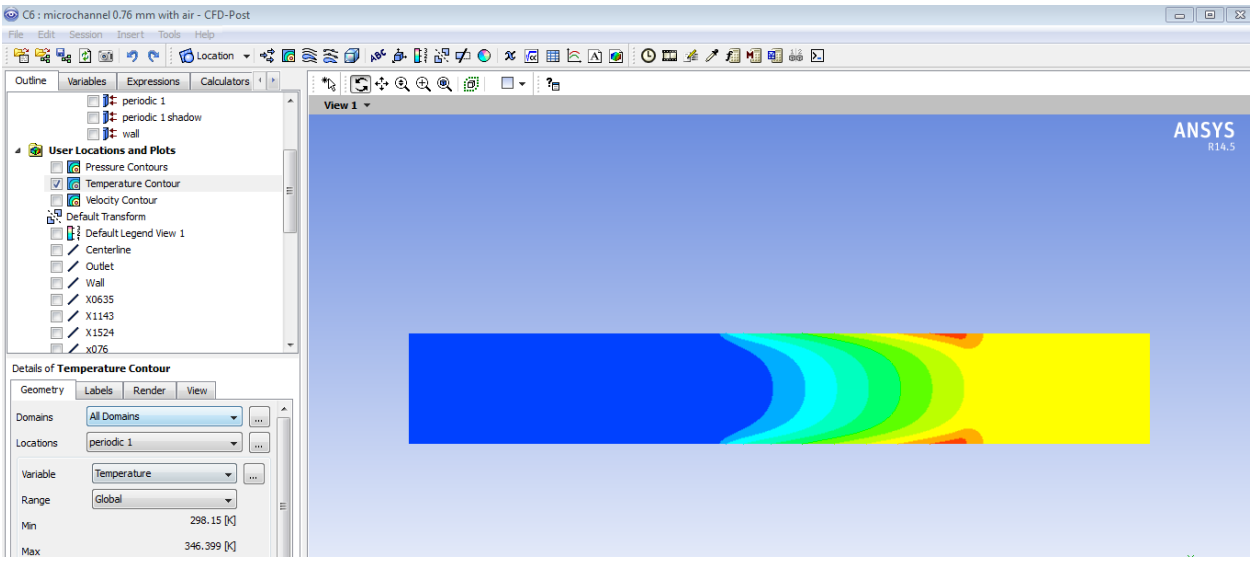

Fig. 6.3 temperature contour

6.5 Pressure Contour

The pressure contour in the present case appears as below:

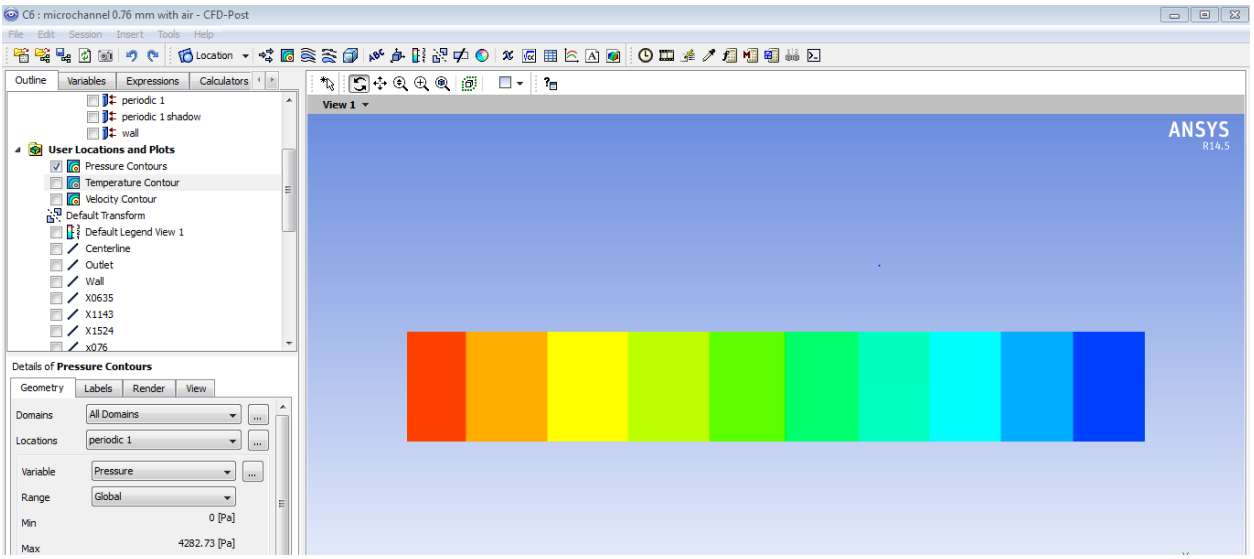

Fig. 6.4 pressure contour

Pressure decreases in the direction of flow with the maximum and minimum value in gauze scale being 4282.73 Pa. and zero respectively

6.6 Graph of Temperature along Centerline

The graph of temperature along centerline appears as below:

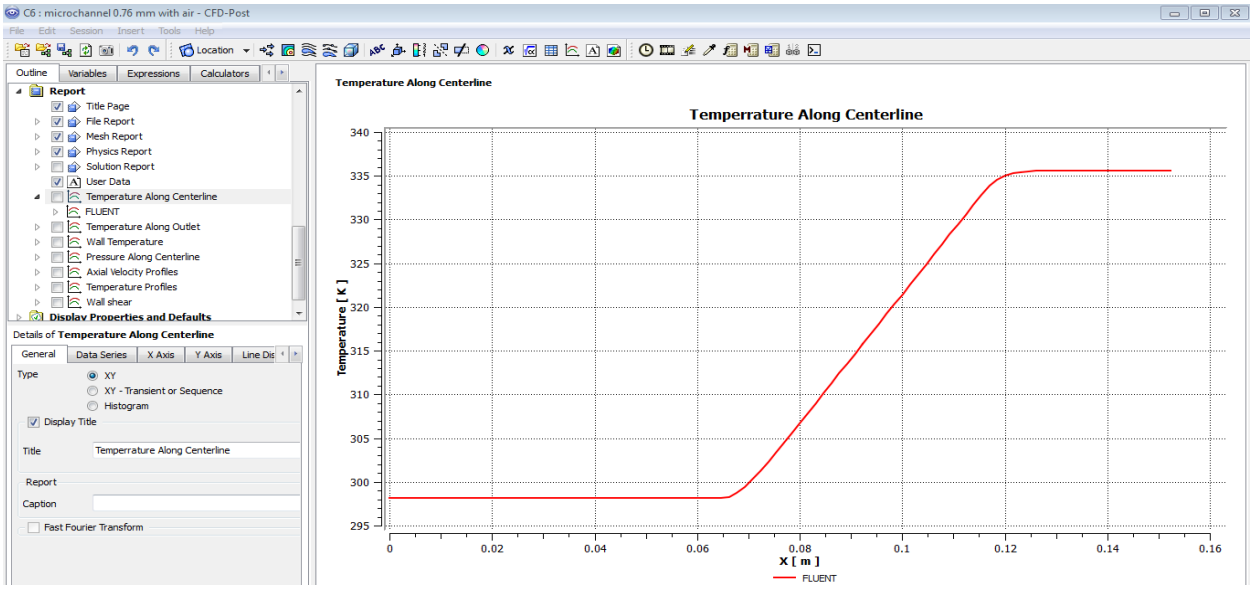

Fig. 6.4 temperature along centerline

Temperature remains constant except for the heating region where it increases uniformly.

6.7 Wall Temperature Variation

Wall temperature graph appears as below:

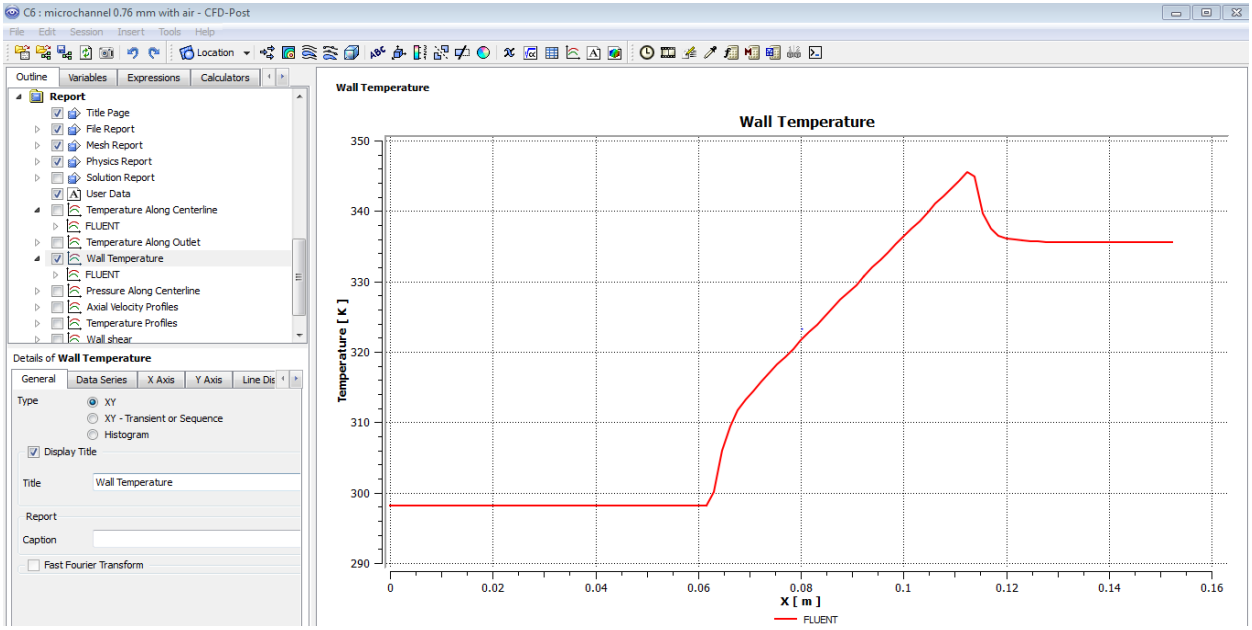

Fig. 6.6 wall temperature variation

Temperature of the channel wall attains the maximum value at the end of heating section i.e; at x=0.1143m.

6.8 Pressure Plot along Centerline

Pressure variation along the centerline appears as below:

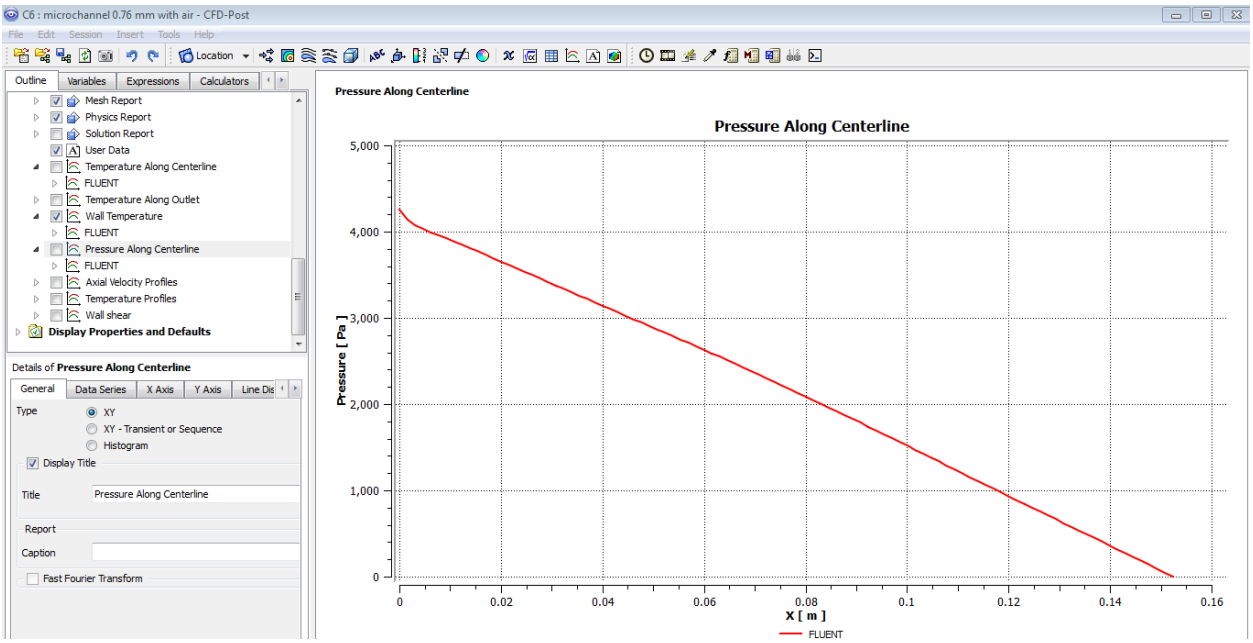

Fig. 6.7 pressure variation along centerline

Pressure decreases continuously from inlet to exit of the channel with the value of zero gauze pressure at the exit.

6.9 Axial Velocity Profile

Axial velocity variation at the three different locations inside the channel namely at x = 0.0635m, x = 0.1143m and x = 0.1542m is plotted. These curves show

variation of axial velocity in Y direction at respective locations. The axial velocity profile appears as below:

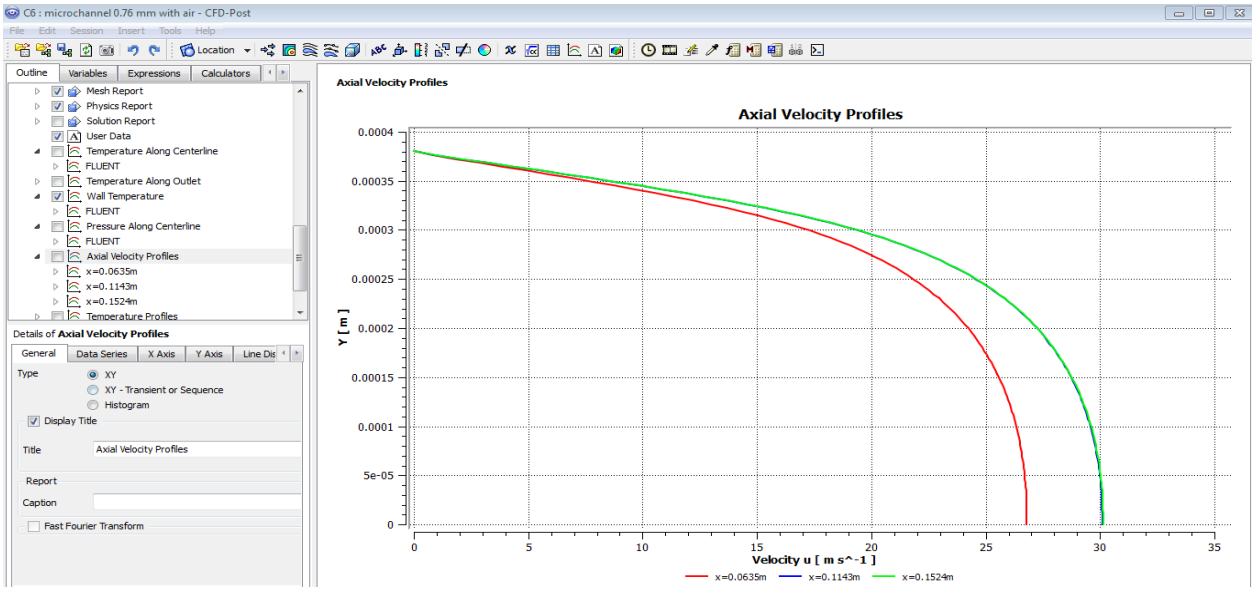

Fig. 6.8 axial velocity profile

Velocity is the maximum at the central axis of the channel irrespective of locations.

6.10 Temperature Profile

The variation in temperature at the same locations as above is drawn which is below:

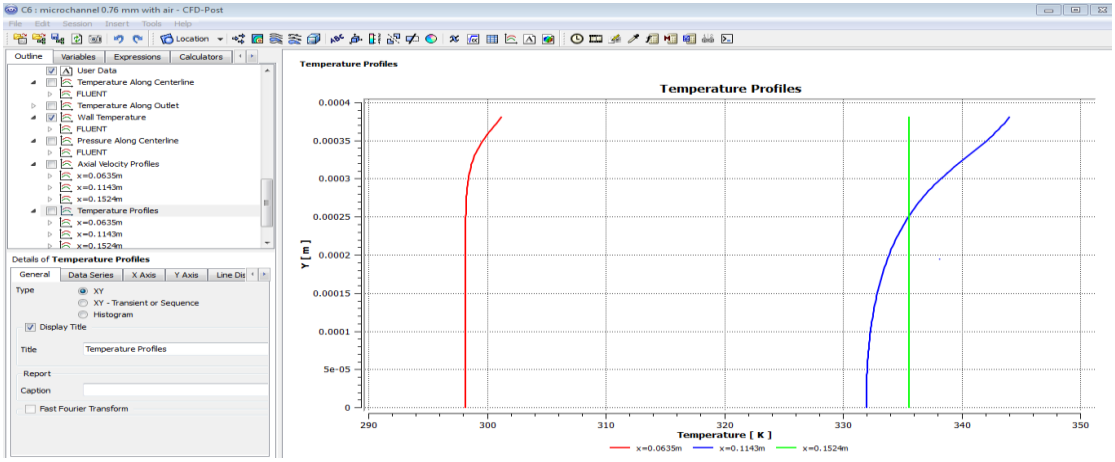

Fig. 6.9 temperature profile

As we move closer to the channel wall temperature rises except for the exit where it is constant.

6.11 Wall Shear Variation

The variation in wall shear in the direction of flow is plotted which appears as below:

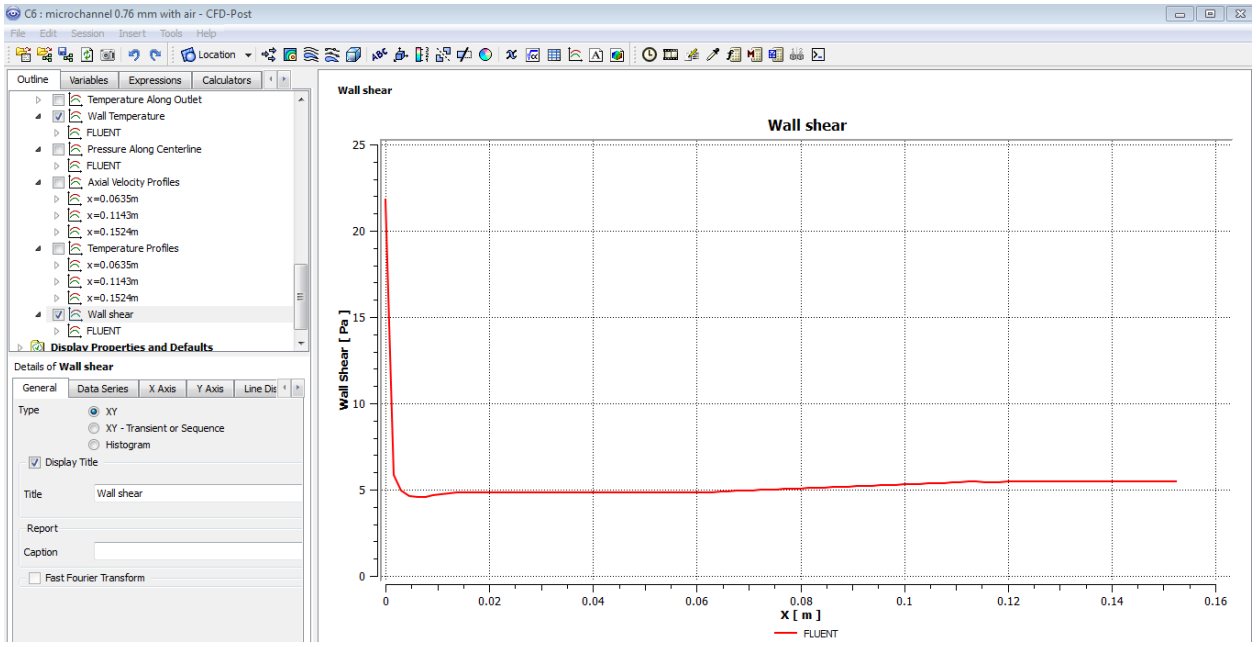

Fig. 6.10 wall shear variation

Wall shear falls and again rises in the flow developing region, then it remains constant when flow is fully developed. In the heated region curve of wall shear rises again the till end of the heated region. After the heated region is over it again remains constant.

7. CONCLUSION

7.1 Conclusions

Result of CFD analysis was validated using results of experimental work of T. A. ADAMS and therefore the model is genuine and can be applied to any fluid flow and heat transfer problem in the circular microchannel. Features of this chapter can be concluded as below:

- Simulation of circular microchannel, of diameter 0.76mm and 1.09mm, with water as a coolant with turbulent flow and forced convective heat transfer subjected to uniform heat flux of 3000 W/m^2, was performed.
- Simulation of microchannel of diameter 0.76mm with air as a coolant was also performed.
- Graphs comparing axial velocity at three different locations namely at x = 0.0635m, x = 0.1143m, x = 0.1542m inside the channel, were plotted. The axial velocity variations in Y direction, in case with water as a coolant overlapped each other but in case of air the variation in axial velocity at different locations were different.
- The maximum temperature attained by the coolant in case of air was 346.399 K while in case of water it was 345.404 K. This is due to fact that water has higher specific heat capacity and thereby more heat carrying capacity.
- Variation in wall shear was plotted in the direction of flow. The plot showing variation in wall shear first fell and then rose a little bit in the region where flow is not fully developed when using water as a coolant. But in case of air as a coolant curve first falls down in the flow developing

region, remains constant once flow is fully developed, rises in the heated region after which it again remains constant.

- Rise in temperature of channel wall is more in case of air when used as a coolant.
- Deviation in value of Nusselt number calculated experimentally, from the values which are predicted from different correlations are more for higher Reynolds number.
- The present analysis shows that water promises to be a better coolant when compared to air.

7.2 Scope of Future Work

- From the analysis of microchannel, it is found that if microchannel is subjected to higher heat flux, temperature of fluid in that case may rise to and above its boiling point. This suggests need of multiphase analysis to predict the performance of microchannel.

- In the heated region temperature of coolant, chip and electronic chip increases in the flow direction. The coefficient of thermal expansion is different for chip and electronic packages. Because of this they are subjected to thermal stress. To overcome this situation a microchannel with two phase flow of the coolant can be utilized. As in case of two phase flow the concept of latent heat may result in uniform temperature distribution on the chip.

8. References:

[1] Qu W, Mudawar, 2002, "Analysis of three-dimensional heat transfer in microchannel heat sinks" *Intenational Journal of Heat and Mass Transfer*, Vol. 45, pp. 3973–85.

[2] C.J.Kroeker, H.M. Soliman, S.J. Ormiston, 2004, "Three-dimensional thermal analysis of heat sinks with circular cooling micro-channels", *International Journal of Heat and Mass Transfer*, Vol. 47, pp. 4733–4744.

[3], [4], [5] Shakuntala Ojha, 2009, " Cfd Analysis on Forced Convection Cooling of Electronic Chips", Department of Mechanical Engineering National Institute of Technology, Rourkela.

[6] Y.S.Muzychka, 2005, "constructal design of forced convection cooled microchannel heat sinks and heat exchanger" *International Journal of Heat and Mass Transfer*, Vol. 48, pp. 3119–3127.

[7] Ravindra Kumar, Mohd. Islam and M.M. Hasan, 2014, "A Review of Experimental Investigations on Heat Transfer Characteristics of Single Phase Liquid Flow in Microchannels" , *International Journal of Advanced Mechanical Engineering*, Vol. 4, pp. 115-120.

[8] Sambhaji T. Kadam, Ritunesh Kumar, 2014, "Twenty first century cooling solution: Microchannel heat sinks", *International Journal of Thermal Sciences*, Vol. 35, pp. 73-92.

[9] Tuckerman, D.B. and Pease, R.F., (1981), "High performance heat sinking for VLSI", *IEEE Electronic Devices Letters*, Vol. 2, pp. 126-129.

[10] Wong, H. and Peck, R.E., (2001), "Experimental evaluation of air-cooling electronics at high altitudes", *ASME Journal of Electronic Packaging*, Vol. 123, pp. 356-365.

[11] Lee, P. and Garimella, S.V., (2003), "Experimental investigation of heat transfer in microchannels", Paper No. HT2003-47293, *ASME Proceedings of HT2003 Summer Heat Transfer Conference*, Vol. 37.

[12] Choi, S.B., Barron, R.F. and Warrington, R.O., (1991), "Fluid flow and heat transfer in microtubes", *ASME Micromechanical Sensors, Actuators, and Systems*, Vol. 32, pp. 123-134.

[13] Rahman, M.M. and Gui, F., (1993), "Experimental measurements of fluid flow and heat transfer in microchannel cooling passages in a chip substrate", *ASME International Electronics Packaging Conference*, Binghamton, New York, USA, Vol. 4, pp. 685-692.

[14] Rahman, M.M. and Gui, F., (1993), "Design, fabrication and testing of microchannel heat sinks for aircraft avionics cooling", *Proceedings of the Intersociety Energy Conversion Engineering Conference*, Vol. 1, pp. 1-6.

[15] Adams, T.M., Abdel-Khalik, S.I., Jeter, S.M. and Qureshi, Z.H., (1998), "An experimental investigation of single-phase forced convection in microchannels", *International Journal of Heat and Mass Transfer*, Vol. 41, pp. 851-857.

[16] M. Mahalingam and J. Andrews, High Performance Air Cooling for Microelectronics, in: Proc. Int. Symp. on Cooling Technology for Electronic Equipment, Honolulu, Hawaii, pp. 608–625, 1987.

[17] S. Yu, T. Ameel, and M. Xin, An Air-Cooled Microchannel Heat Sink with High Heat Flux and Low Pressure Drop, in: Proc. 33-rd Nat. Heat Transfer Conf., Albuquerque, New Mexico, Paper No. NHTC 99-162, pp. 1–7, 1999.

[18] A. Aranyosi, L. M. R. Bolle, and H. A. Buyse, Compact Air-Cooled Heat Sinks for Power Packages, IEEE Trans. Components, Pack. Manuf. Technol. Part A, Vol. 20, pp. 442–451, 1997.

[19] Peng, X.F. and Peterson, G.P., (1996), "Concective heat transfer and flow friction for
water flow in microchannel structures", *Intenational Journal of Heat and Mass Transfer*,
Vol. 39, pp. 2599-2608.

[20] Mokrani, O., Bourouga, B., Castelain, C. and Peerhossaini, H. 2009. "Fluid flow and
convective heat transfer in flat micro channels, *International Journal of Heat and Mass
Transfer*, Vol. 52, pp. 1337–1352.

[21] C.J. Kroeker, H.M. Soliman , S.J. Ormiston, 2004, "Three-dimensional thermal analysis of heat sinks with circular cooling micro-channels", *International Journal of Heat and Mass Transfer,*Vol. 47, pp. 4733–4744.

[22] Reiyu Chein, Janghwa Chen, 2009," Numerical study of the inlet/outlet arrangement effect on microchannel heat sink performance", *International Journal of Thermal Sciences,* Vol. 48, pp. 1627–1638.

[23] H. Ghaedamini, P.S. Lee , C.J. Teo, 2013, "Developing forced convection in converging–diverging microchannels", *International Journal of Heat and Mass Transfer,* Vol. 65, pp. 491-499.